Provided for non-commercial research and education use.
Not for reproduction, distribution or commercial use.

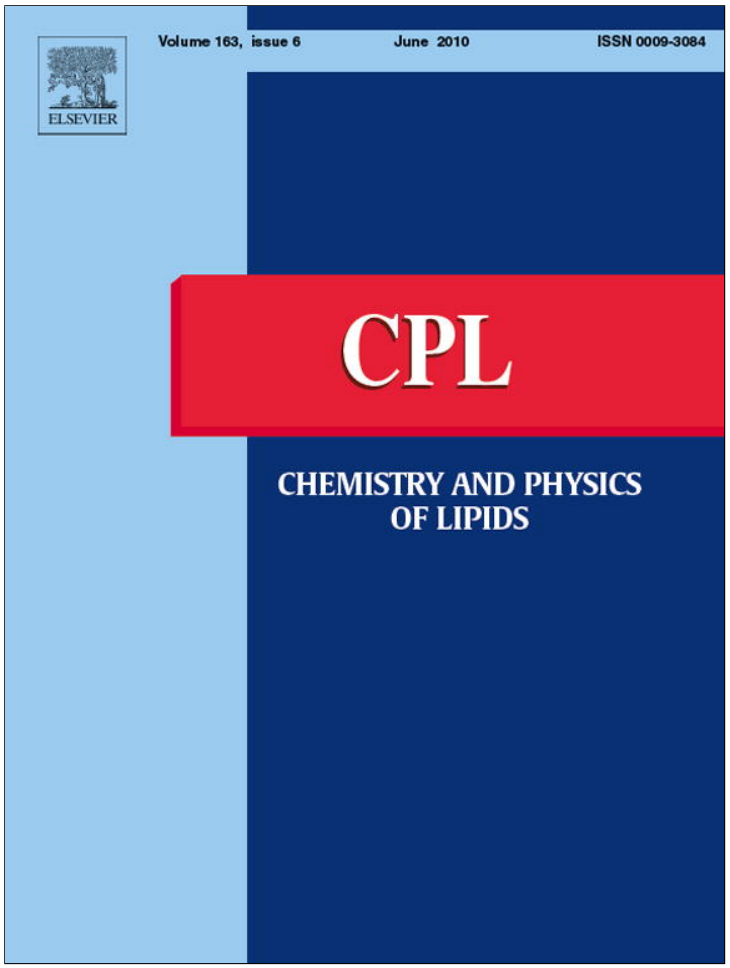

This article appeared in a journal published by Elsevier. The attached copy is furnished to the author for internal non-commercial research and education use, including for instruction at the authors institution and sharing with colleagues.

Other uses, including reproduction and distribution, or selling or licensing copies, or posting to personal, institutional or third party websites are prohibited.

In most cases authors are permitted to post their version of the article (e.g. in Word or Tex form) to their personal website or institutional repository. Authors requiring further information regarding Elsevier's archiving and manuscript policies are encouraged to visit:

http://www.elsevier.com/copyright

Author's personal copy

Chemistry and Physics of Lipids 163 (2010) 460–479

Contents lists available at ScienceDirect

Chemistry and Physics of Lipids

journal homepage: www.elsevier.com/locate/chemphyslip

Review

Applications of neutron and X-ray scattering to the study of biologically relevant model membranes

G. Pabst[a], N. Kučerka[b,c], M.-P. Nieh[b], M.C. Rheinstädter[b,d], J. Katsaras[b,e,f,*]

[a] Institute of Biophysics and Nanosystems Research, Austrian Academy of Sciences, A-8042 Graz, Austria
[b] Canadian Neutron Beam Centre, Steacie Institute for Molecular Sciences, National Research Council, Chalk River, ON K0J 1J0, Canada
[c] Department of Physical Chemistry of Drugs, Faculty of Pharmacy, Comenius University, 832 32 Bratislava, Slovakia
[d] Department of Physics & Astronomy, McMaster University, Hamilton, ON L8S 4M1, Canada
[e] Department of Physics, Brock University, St. Catharines, ON L2S 3A1, Canada
[f] Guelph-Waterloo Physics Institute and Biophysics Interdepartmental Group, University of Guelph, Guelph, ON N1G 2W1, Canada

ARTICLE INFO

Article history:
Received 27 January 2010
Received in revised form 23 March 2010
Accepted 24 March 2010
Available online 31 March 2010

Keywords:
Lipid bilayers
Phosphorylcholine
Cholesterol
Bicelles
Bending modulus
Neutron and X-ray diffraction
SANS and SAXS
Membrane dynamics
Inelastic neutron scattering

ABSTRACT

Scattering techniques, in particular electron, neutron and X-ray scattering have played a major role in elucidating the static and dynamic structure of biologically relevant membranes. Importantly, neutron and X-ray scattering have evolved to address new sample preparations that better mimic biological membranes. In this review, we will report on some of the latest model membrane results, and the neutron and X-ray techniques that were used to obtain them.

Crown Copyright © 2010 Published by Elsevier Ireland Ltd. All rights reserved.

Contents

1. Introduction 461
   1.1. Membranes 461
   1.2. Neutron and X-ray diffraction 462
2. Contrast variation in X-ray and neutron diffraction studies 462
   2.1. Anomalous X-ray scattering 462
   2.2. Isotopic substitution in neutron scattering studies 463
3. Determination of a membrane's elastic properties 464
4. Determining the forces between membranes 466
5. Membrane structure 467
   5.1. Single component membranes 468
   5.2. Lipid mixtures and domains 469
   5.3. "Bicelle" mixtures: resultant morphologies 471
6. Membrane active compounds 472
   6.1. Effect of peptides on bilayer properties 472
   6.2. Ion-specific effects 472
7. Membrane dynamics 473
   7.1. Inelastic neutron scattering 474

* Corresponding author. Tel.: +1 613 584 8811x3984; fax: +1 613 584 4040.
E-mail address: John.Katsaras@nrc.gc.ca (J. Katsaras).

0009-3084/$ – see front matter. Crown Copyright © 2010 Published by Elsevier Ireland Ltd. All rights reserved.
doi:10.1016/j.chemphyslip.2010.03.010

Author's personal copy

7.2. Interactions in membranes 474
8. Concluding remarks 475
References 475

1. Introduction

1.1. Membranes

Throughout the biological world cell membranes are crucial to the life of individual cells. In animal cells the plasma membrane surrounding the cell is a selectively permeable barrier made up primarily of proteins and lipids, and separates the cytosol from the extracellular environment (Fig. 1). Membranes also surround the various cell organelles (e.g. mitochondria, endoplasmic reticulum, Golgi apparatus, etc.), enabling them to maintain their characteristic differences from the cytosol. Besides serving as a selective permeability barrier, the plasma membrane acts as an anchor for the cytoskeleton, a cellular network of fibres contained within the cytoplasm that imparts to the cell, structure, shape and movement.

It was not until the early 1970s that membranes were recognized as being two-dimensional (2D) liquids, where individual lipid molecules, for the most part, diffuse freely within the 2D plane (Singer and Nicolson, 1972). We now know that lipids and proteins are not randomly distributed in the plasma membrane, but in some cases may form functional domains. The existence of functional domains was first demonstrated by Goodsaid-Zalduondo et al. (1982), and later by Simons and van Meer (1988) using a combination of cell membrane lipids (i.e. glycolipids, sphingolipids and cholestrol). For the most part, functional domains can be classified as: (a) protein–protein complexes (e.g. Pawson and Nash, 2003; Gavin and Superti-Furga, 2003; Betts and Russell, 2007); (b) lipid rafts (e.g. Jacobson and Dietrich, 1999; McIntosh, 2007); and (c) pickets and fences formed by the cytoskeleton. (e.g. Abbott, 2005; Nakada et al., 2003).

Despite their different functions, all membranes are asymmetric (i.e. different molecular composition between the bilayer's two leaflets), non-covalent assemblies consisting of a thin layer of lipid and protein molecules. The amphipathic lipid molecules spontaneously arrange themselves in so-called bilayers (Fig. 1), whereby their hydrophobic "tails" are shielded from the surrounding water, while exposing their hydrophilic "headgroups" to the cytoplasmic and extracellular spaces. Essentially, this lipid bilayer structure was first proposed in 1925 by Gorter and Grendel (1925) using an apparatus similar to what we now know as a Langmuir trough – originally developed by Pockels (1894) and later improved by Langmuir (1917). Effectively, they demonstrated that lipids extracted from red blood cells occupied approximately twice the cell's surface area.

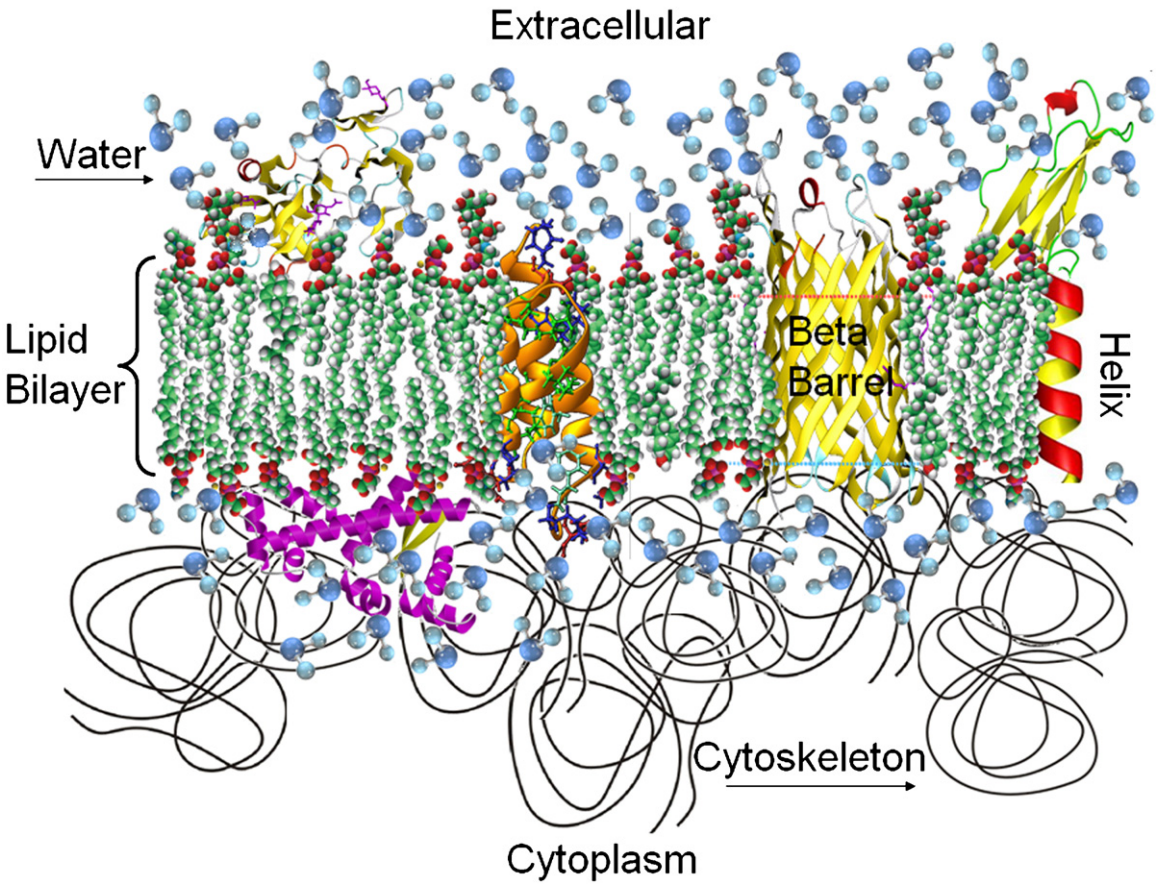

Fig. 1. Cartoon of a cell or plasma membrane, a selectively semi permeable barrier separating the cell's contents (cytoplasm) from its outside environment. The plasma membrane contains a wide variety of molecules, primarily proteins and lipids, the amounts which differ between species and a cell's function. Protein functions include signalling, cell-cell communication, enzymatic activity, transport, etc. Cell membranes consist of three classes of lipids (i.e. phospholipids, glycolipids and steroids) whose amounts, similar to proteins, differ depending on cell type. The cytoskeleton is a protein found in all cells which, among other functions, maintains a cell's shape and plays an important role in cell division.

Author's personal copy

In the 1960s Chapman et al. (1966) demonstrated the existence of thermotropic phase transitions in anhydrous lipids and lipid/water systems (Chapman and Fluck, 1966; Chapman and Morrison, 1966; Chapman et al., 1967, 1974). Chapman and Salsbury (1966), and were the first to show the distribution of motions along the fatty acid chains in phosphatidylethanolamine (PE) bilayers in the now commonly known liquid crystalline phase (L_α). It was noted that these translational and rotational movements were particularly accentuated in the fatty acid chain's terminal methyl group.

In the early 1970s Tardieu et al. (1973) published an X-ray study in which almost all of the known lamellar phases assumed by pure lipid/water systems were identified. In many fully hydrated di-saturated phosphatidylcholines (PCs), such as dipalmitoyl PC (DPPC, 16:0-16:0 PC), on decreasing temperature there exist three lamellar phases (i.e. L_α, $P_{\beta'}$ and $L_{\beta'}$) differing primarily in the "order" of their hydrocarbon chains. For example, the fatty acid chains in L_α bilayers are in a "melted" state possessing no long-range order within the 2D lipid bilayer matrix. On the other hand, $L_{\beta'}$ bilayers are characterized by a 2D ordering of their tilted hydrocarbon chains (Chapman et al., 1967). In fact, depending on the degree of hydration the hydrocarbon chains of $L_{\beta'}$ bilayers differ in the direction of their molecular tilt with respect to the 2D bond direction, i.e. nearest neighbour or next nearest neighbour interactions (Smith et al., 1988). Although the in-plane hydrocarbon chain arrangement is nearly hexagonal, it does not imply a regular packing of the lipid molecules themselves. In fact, analysis of the diffuse X-ray scattering from $L_{\beta'}$ bilayers indicates a large degree of headgroup disorder (Sun et al., 1994), as is the case for L_α and $P_{\beta'}$ bilayers. Things are very different, however, in the case of subgel or $L_{c'}$ bilayers.

The $L_{c'}$ phase was first observed by Chen et al. (1980) using differential scanning calorimetry (DSC) after incubating DPPC bilayers for a few days at ~0 °C. A few years later Ruocco and Shipley (1982a,b) first characterized the packing of the hydrocarbon chains in $L_{c'}$ DPPC bilayers, and Blaurock and McIntosh (1986) did the same for dipalmitoyl phosphosphatidylglycerol (DPPG, 16:0-16:0 PG). However, despite numerous studies, the overall structure of $L_{c'}$ bilayers was not resolved until aligned multibilayer stacks were prepared (Raghunathan and Katsaras, 1995; Katsaras et al., 1995). It was demonstrated that on decreasing temperature the $L_{\beta'}$ to $L_{c'}$ transition resulted in the lipid molecules (PC headgroups) becoming ordered in the plane of the bilayer. Interestingly, this ordering took place without destroying the hydrocarbon chain lattice. The implication of this result was that the simultaneous existence of the two lattices required the molecular lattice to be a superlattice of the chain lattice – effectively a disorder–order transition, where the normally disordered PC headgroups order forming a 2D lattice, and similar to the case of subgel DPPG bilayers (Blaurock and McIntosh, 1986). Moreover, the molecular lattices were found to be positionally correlated across the same bilayer (i.e. intra bilayer), even though there was no evidence of inter bilayer correlations (Raghunathan and Katsaras, 1995; Katsaras et al., 1995). Subsequently, the structure of oriented $L_{c'}$ bilayers was used to reanalyze the powder diffraction data of a number of hydrated lipids possessing PC headgroups (Raghunathan and Katsaras, 1996). Without exception, the systems were all characterized by the 2D ordering of their lipid molecules.

In addition to the lamellar phases discussed, lipid/water dispersions form a variety of other structures, primarily hexagonally arranged rods (hexagonal H_I) and tubes (inverted hexagonal H_{II}), and bicontinuous 3D structures with cubic symmetries (for a review see Rappolt, 2006). In particular, cubic phase lipids have been used as of late to solve the structures of difficult to crystallize integral membrane proteins which comprise a large proportion of the genome (Lundstrom, 2004; Cherezov et al., 2006; Lundstrom, 2006). Introduced by Landau and Rosenbusch (1996), this method of protein crystallization was employed to solve the structure of bacteriorhodopsin (bR) using the microcrystals grown in a monoolein-based cubic phase (Pebay-Peyroula et al., 1997; Luecke et al., 1998, 1999a; Belrhali et al., 1999). In this bicontinuous lipid phase matrix, the proteins are encased in a natural bilayer environment, yet they are allowed to diffuse throughout the sample creating crystal nuclei. Functionally, these microcrystals have been shown to be indistinguishable from bR in native purple membrane (PM) as both samples underwent the identical photocycle upon photoexcitation (Heberle et al., 1998). This method of crystallization has also proven to be effective in crystallizing small molecules and water-soluble proteins (Landau et al., 1997; Rummel et al., 1998).

1.2. Neutron and X-ray diffraction

Neutron and X-ray scattering have proven to be two of the most powerful structural determination techniques. In particular, X-ray crystallography has been successfully applied to solving the crystal structures of proteins, beginning in the late 1950s with the structure of sperm whale myoglobin (Kendrew et al., 1958). Since then, according to the RCSB Protein Data Bank, more than 60,000 crystal structures of proteins and other biological molecules have been determined, with X-ray crystallography accounting for the vast majority of the structures – nuclear magnetic resonance (NMR) techniques have solved approximately 7500 structures, usually of molecular weight less than 70 kDa.

Neutron and X-ray scattering are similar in that both techniques are capable of providing dynamical and structural information. However, whereas X-rays are scattered primarily by electrons, neutrons are fundamental particles scattered primarily by their interaction with atomic nuclei. Although the scattering "ability" of X-rays increases in a simple way with atomic number, in the case of neutron scattering this depends in a complex manner on the nucleus' mass, spin and energy levels. Since neutrons interact uniquely with different nuclei, including with the various isotopes of elements, this fashion of neutrons interacting with atoms allows for the powerful and commonly used contrast variation method. In the case of biological samples inherently rich in hydrogen (^1H), the classic example is the substitution of ^1H for its isotope deuterium (^2H). This method for selectively tuning the sample's "contrast" is used to accentuate or nullify the scattering from particular regions of a macromolecular complex.

With regards to structural biology, the various neutron (Fitter et al., 2006) and X-ray scattering techniques complement crystallographic studies that require hard to obtain high quality crystals of macromolecules. Importantly, small angle neutron (SANS) and X-ray scattering (SAXS) are ideally suited to studying biomolecules and their assemblies in solution, including molecules whose crystallization conditions have yet to be determined. In addition, neutron and X-ray reflectometry have emerged as powerful surface/interface probes used to characterize the structures of materials on solid and fluid planar surfaces (e.g. Krueger, 2001; McGillivray et al., 2007; Horton et al., 2007). The most commonly used approach being specular reflectivity, a technique that measures the scattering density profile perpendicular to the sample's adsorbed surface.

2. Contrast variation in X-ray and neutron diffraction studies

2.1. Anomalous X-ray scattering

Synchrotron radiation has enabled the technique of anomalous X-ray scattering to impact a number of areas of science, especially

Author's personal copy

biology, as it facilitates the structural determination of proteins and other biological macromolecules. For example, selenium is used to replace sulphur containing amino acids. By "tuning" the synchrotron energy to the absorption edge of selenium, the scattering from selenium is altered highlighting that particular element (i.e. contrast variation). Moreover, the ubiquitous "phase problem" (encountered in all of scattering) can be solved by utilizing different wavelength X-rays that are easily produced by synchrotrons, eliminating the traditional preparation of difficult to produce heavy atom derivatives that have traditionally been used for structural determination (Ealick, 2000). This technique of solving the phase problem is known as multiple wavelength anomalous diffraction, or MAD for short.

In the case of X-ray diffraction, the phase problem with regards to biological membranes and model systems has been solved using a number of techniques (e.g. Akers and Parsons, 1970; Luzzati et al., 1972; Torbet and Wilkins, 1976; Franks, 1976; Franks et al., 1978). However, there have only been a few occasions where MAD has been used to solve the structure of a model membrane system (e.g. Liu et al., 1991; Pan et al., 2006). For example, MAD was used to elucidate the structure of membranes containing gramicidin ion channels with bound thullium ions, whose absorption edges (i.e. of thullium) were used to determine the membrane-active structure of this antibiotic peptide (Liu et al., 1991). In the recent past, MAD was used to determine the structure of an inverted hexagonal phase made up of phospholipids with brominated fatty acid chains (Pan et al., 2006). This study was of general interest, as hydrophobic interstices are believed to occur during membrane fusion with the inverted hexagonal phase possibly being such an intermediate phase. Importantly, Pan et al. (2006) determined that lipid hydrophobic chains pack in a hexagonal unit cell with each hydrocarbon chain occupying the same volume, irrespective of the degree of chain stretching.

2.2. Isotopic substitution in neutron scattering studies

Neutron scattering lengths are different for isotopes of the same element. This is because neutron scattering is the result of nuclear forces and the neutron scattering length can experience a dramatic change in magnitude and phase as a result of resonance scattering. Importantly, in the case of hydrogen its scattering length is negative even at energies far from its resonance energy. In the case of biological material inherently rich in hydrogen, dramatic changes in scattering amplitudes are achieved through the substitution of ^{1}H for its isotope ^{2}H, selectively tuning the sample's contrast (Jacrot, 1976). Over the years, this technique of isotopic substitution has been used to study viruses (Jacrot, 1976; Cusak et al., 1985), proteins (Satre and Zaccai, 1979; Zaccai, 2000a,b), DNA/RNA structure (Parfait et al., 1978; Hammermann et al., 1998; Ledere et al., 2005), and model membranes (Zaccai et al., 1975, 1979; Büldt et al., 1978; Léonard et al., 2001). An example where isotopic substitution was used, and that has attracted some attention, is the bilayer system made up of lipids with polyunsaturated fatty acid (PUFA) chains (20:4-20:4) and the location of cholesterol therein (Harroun et al., 2006, 2008; Marrink et al., 2008) – some of the earliest diffraction studies of cholesterol in lipid bilayers are the pioneering works of Franks (1976), and Worcester and Franks (1976).

Cholesterol and saturated lipid species preferentially partition into liquid ordered microdomains (e.g. lipid rafts), away from unsaturated lipid species. Harroun et al. (2006, 2008) explored the effect of unsaturation upon the orientation of cholesterol using aligned multibilayer stacks of cholesterol in PC bilayers with varying amounts of acyl chain unsaturation. Specifically, deuterated "headgroup" or "tailgroup" cholesterol (Fig. 3) was used to provide the necessary contrast. As mentioned, the technique relies on the specific deuterium labeling of molecular groups, the unique ability of neutrons to distinguish between hydrogen and deuterium atoms, and the Fourier reconstruction of the bilayer profile from the diffraction data. Subtracting the unlabeled sample data from the deuterium labeled data results in the location of the label (Fig. 4).

Harroun et al. (2006) located cholesterol's headgroup (i.e. 2,2,3,4,4,6-D6) to reside approximately 16 Å from the middle of 1-palmitoyl-2-oleoyl PC (16:0-18:1 PC, POPC), 1,2-dioleoyl PC (18:1-18:1 PC, DOPC) (Fig. 4a), and 1-stearoyl-2-arachidonyl PC (18:0-20:4 PC) bilayers. This location placed cholesterol's hydroxyl group close to the membrane surface, indicative of the molecule in its commonly observed "upright" (e.g. Franks, 1976; Worcester and Franks, 1976; Léonard et al., 2001) orientation (Fig. 2a). In the case

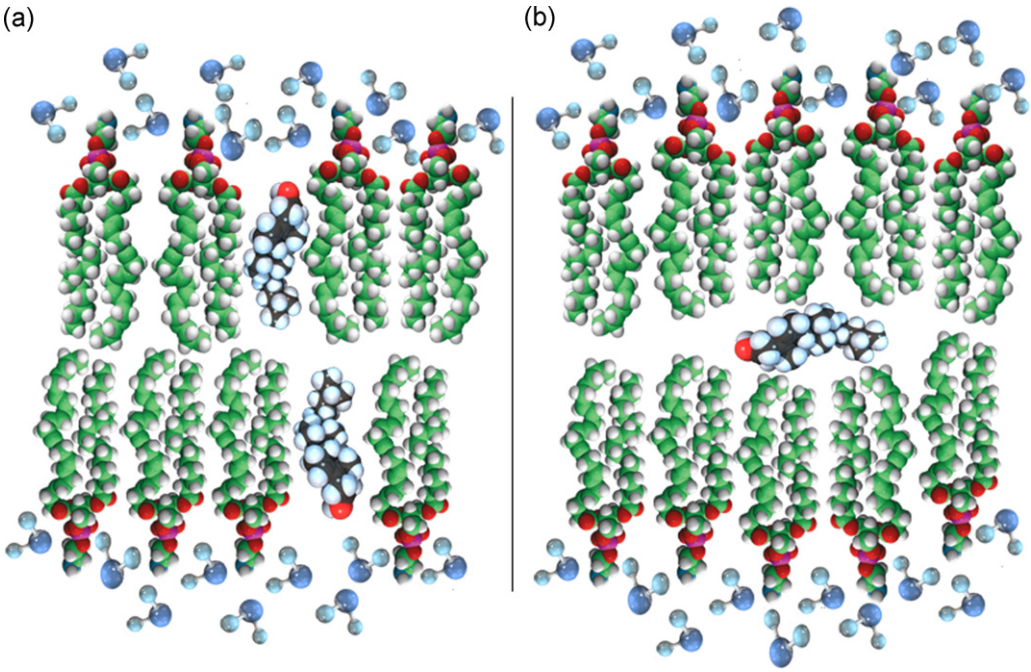

Fig. 2. a) Lipid bilayers showing cholesterol in its "upright" orientation and b) lying flat in the bilayer center.

Author's personal copy

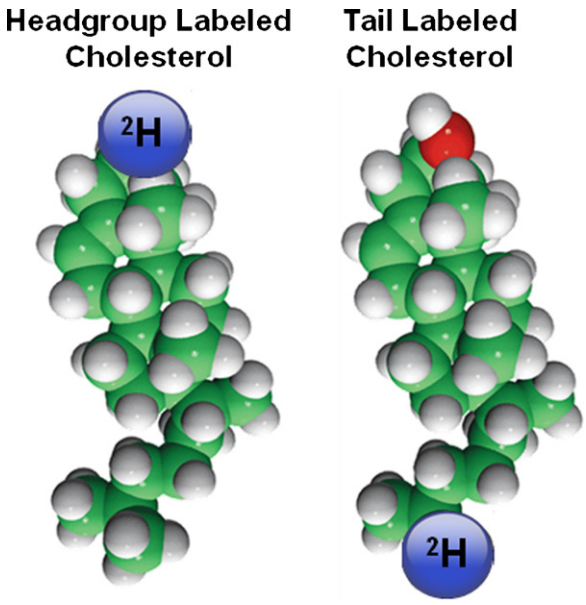

Fig. 3. "Headgroup" (2,2,3,4,4,6-D6) and "tail" (25,26,26,26,27,27-D7) deuterium labeled cholesterol.

of PUFA (20:4-20:4 PC) bilayers, however, the hydroxyl group of headgroup labeled cholesterol was found sequestered in the bilayer center (Fig. 3a). From their initial study the unresolved question was whether the molecule was inverted or lying flat in the middle of the bilayer. This question was subsequently resolved using tail labeled (i.e. 25,26,26,26,27,27-D7) cholesterol (Fig. 3), unequivocally demonstrating cholesterol's ability to sequester itself in the middle of 20:4-20:4PC bilayers (Fig. 4B) (Harroun et al., 2008).

The experimental data by Harroun et al. (2006, 2008) were revisited by Marrink et al. (2008) using the MARTINI coarse grained (CG) model to simulate the behavior of cholesterol in different lipid bilayers. The MARTINI model groups atoms into CG beads allowing for simulation times in the microsecond range, while practically retaining atomic resolution detail. Interestingly, the CG simulations found cholesterol undergoing rapid flip-flop between the bilayer's two leaflets, but spending a considerable amount of time in the membrane's interior, consistent with the neutron scattering data.

Recently, Kučerka et al. (2009a) demonstrated cholesterol's preference to different lipids, namely POPC and dimyristoyl PC (14:0-14:0 PC, DMPC). By "titrating" POPC into PUFA bilayers, it was observed that it took approximately 50 mol% of POPC to induce cholesterol to revert to its upright orientation (Fig. 2a), while only 5 mol% of DMPC was needed to achieve the same result. The authors noted that the mole ratio of DMPC required to flip cholesterol in PUFA bilayers was approximately 2 cholesterols per DMPC, a mole ratio that corresponds to the maximum solubility of cholesterol in PC bilayers (Huang et al., 1999). Moreover, the data by Kučerka et al. (2009a) agree with the umbrella model (Huang and Feigenson, 1999) that hypothesized that 1 DMPC molecule is capable of shielding 2 cholesterol molecules from water, thus reducing the energy penalty and enabling cholesterol to assume an upright orientation in PUFA lipid bilayers.

3. Determination of a membrane's elastic properties

Fully hydrated liquid crystalline samples are generally assumed to best mimic physiologically relevant conditions. However, these disordered bilayers do not diffract well (i.e. give rise to a limited number of quasi-Bragg peaks), and as such do not lend themselves ideally to traditional crystallographic analysis. On the other hand, the scattering patterns from these thermally fluctuating bilayers contain diffuse scattering information which can be analyzed to reveal previously hard to obtain information regarding bilayer structure and interactions.

In 1972 Caillé (1972) predicted power law line shapes to describe the diffraction maxima from smectic liquid crystals. Importantly, he related the derived exponents to material properties, such as the bending modulus K_C of a single bilayer and the bulk compression modulus B, which describes the interactions between two interacting lipid bilayers. Subsequently, Caillé's theory was altered (modified Caillé theory or MCT) by Zhang et al. (1994) to enable it to predict the line shapes of all diffraction peaks by incorporating into the theory the average correlation length contributing to the scattering. The experimentally obtainable Caillé parameter relates to K_C and B as follows:

$$\eta = \frac{k_B T}{8\sqrt{BK_C}} \frac{4\pi}{d^2}, \tag{1}$$

where k_B is the Boltzmann constant, T the temperature, and d the average lamellar repeat spacing. K_C and B can also be related to the in-plane correlation length (Lei et al., 1995) by:

$$\xi^4 = \frac{K_C}{B}, \tag{2}$$

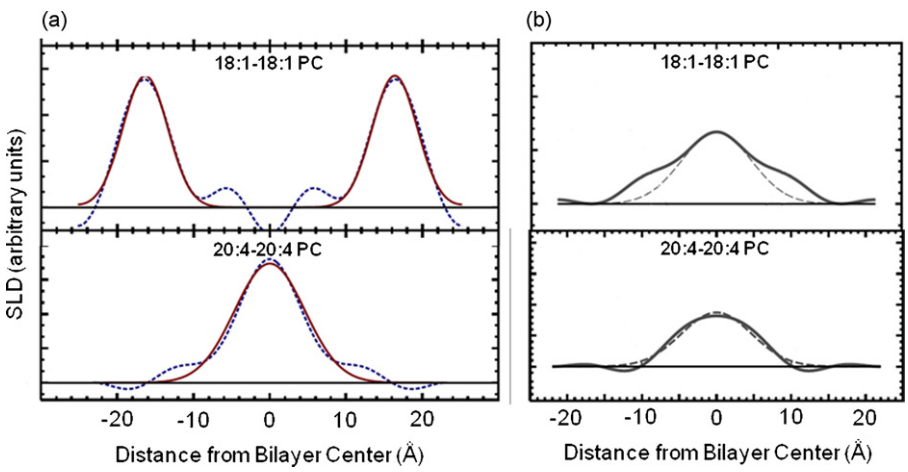

Fig. 4. Scattering length density difference profiles of a) "headgroup" labeled and b) "tail" labeled cholesterol in 18:1-18:1 PC (POPC) and 20:4-20;4 PC bilayers. The dashed lines are Gaussian fits to the data, determining the location of the deuterium labels (adapted from Harroun et al., 2006, 2008).

Author's personal copy

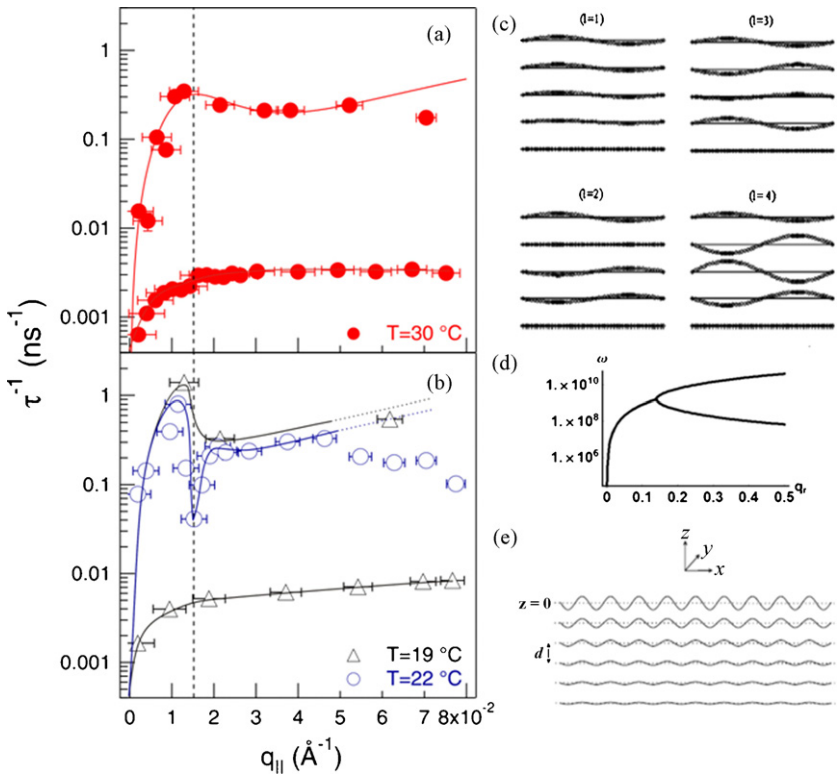

Fig. 5. a) Dispersion relations of fluid phase bilayers at 30 °C. The solid line is a fit to the data using Eq. 3 (Rheinstädter et al., 2006a). b) Dispersion relations in the gel (19 °C) and in the range of critical swelling (22 °C) as adapted from Rheinstädter et al. (2006a). A pronounced soft mode is observed at $q_0 = 0.015$ Å^{-1} at 22 °C, as indicated by the dotted vertical line. c) Fluctuation spectrum of solid supported multilamellar membranes (Romanov and Ul'yanov, 2002), and d) the corresponding analytical dispersion relation. e) The surface mode that is responsible for the slow relaxation branch in parts a) and b) (Bary-Soroker and Diamant, 2006, 2007).

where ξ^2 is the product of d and the de Gennes penetration length Λ (de Gennes and Prost, 1993). Unlike powder samples, where only the Caillé parameter η is obtainable and which contains the product of the material moduli K_C and B, aligned samples offer the possibility of individually determining K_C and B. This was first recognized by Lyatskaya et al. (2001) who determined the material properties of fully hydrated DOPC bilayers – an analogous approach was later conceived by Salditt (2005) using non-specular scattering information at fixed angles of incidence, instead of integrating over all incident angles for a given wave vector. It should be noted, however, that the production of multibilayers is not always possible. For example, natural membranes under physiologically relevant conditions usually contain charged lipid species and are hydrated in an electrolytic environment. Both contributions lead to an electrostatic repulsion between adjacent membranes making it practically impossible to form a fully hydrated multilamellar assembly. One can of course screen the electrostatic repulsion using counterions, however, doing so also influences membrane properties, even if the bilayer is composed entirely of neutral lipids (Pabst et al., 2007c). Although in recent years there have been a number of studies that have analyzed the anisotropic diffuse scattering from aligned samples (e.g. Lyatskaya et al., 2001; Liu and Nagle, 2004; Salditt, 2005; Kučerka et al., 2005; Pan et al., 2008a), previously Pabst et al. (2000) using a modified Caillé structure factor in combination with a Gaussian representation for the one-dimensional (1D) electron density profile (EDP), were able to obtain detailed structural information from fully hydrated POPC and DPPE (16:0-16:0 PE) bilayers.

This approach in analyzing data has been applied to the much studied "anomalous swelling" phenomenon taking place in multibilayer systems near the main transition temperature T_M (e.g. Mason et al., 2001). As the temperature decreases toward T_M, the d-spacing in liquid crystalline bilayers increases. However, only half of this increase was initially attributed to a change in bilayer thickness. Pabst et al. (2003) studied the temperature dependence of the bilayer's elastic properties by analyzing the diffuse scattering from DMPC multilamellar vesicles (MLVs) in order to determine the bilayer's bending modulus K_C (which governs bilayer fluctuations) from the measured Caillé fluctuation parameter. However, since the Caillé parameter is the product of the interbilayer compression B and K_C, additional osmotic pressure experiments were needed in order to estimate their individual contributions. The analysis of the diffuse scattering from oriented samples confirmed that the anomalous swelling which takes place in a certain class of lipid bilayers was the result of bilayer "softening" (see Sections 4 and 7) (Pabst et al., 2003; Chu et al., 2005).

The mesoscopic scale fluctuations that are used to determine B and K_C occur in the nanosecond time range. As such, another approach that is used to determine these moduli is to directly measure their corresponding fluctuation frequencies as a function of the scattering vector q. This can be achieved through the neutron spin-echo technique which is capable of probing nanometer length scales and nanosecond dynamics (see Section 7). Spin-echo offers extremely high energy resolution through the Larmor "tagging" of neutrons, and is in essence a measurement of neutron polarization (Mezei, 1980). In fact, the intermediate scattering function $S(q,t)$ can be used to determine elastic properties (i.e. B and K_C) of membranes.

The spin-echo technique was first applied to biologically relevant materials by Rheinstädter et al. (2006a). Fig. 5a and b show the dispersion relations τ^{-1} vs. q at three different temperatures, namely 19, 22 and 30 °C, where DMPC bilayers are in the gel phase ($P_{\beta'}$), in the region of anomalous swelling (slightly above T_M) (Mason et al., 2001; Pabst et al., 2003), and in the fluid L_α phase, respectively. Two relaxation processes, one at about 10 ns (τ_1) and a second, slower process at about 100 ns (τ_2) were observed, with both relaxation branches being dispersive. The fast process

Author's personal copy

shows $q_{||}{}^2$ increasing at small $q_{||}$ values, but begins to decrease at $q_{||} \sim 0.015\,\text{Å}^{-1}$. The dispersion in the gel phase (19 °C) and close to the phase transition (Fig. 5b) appears to be more pronounced than the 30 °C dispersion. In addition, a soft mode seems to be present at 22 °C, indicating a significant softening of the bilayer in the range of critical swelling at a well-defined wave number. The slow branches at 19 and 30 °C also show increasing relaxation rates with increasing $q_{||}$-values, but with a distinct non-polynomial behaviour.

The dispersion relation of the fast branch with relaxation rates between 1 and 10 ns can be attributed to undulation dynamics. The fluctuation spectrum of solid supported membranes was analytically modeled (Romanov and Ul'yanov, 2002) and is shown in Fig. 5c. Quasi-acoustic (quasi because the modes are not propagating due to the solid support) and optical modes were found with increasing fluctuation amplitudes towards the middle of the membrane stack. The calculated dispersion for the quasi-acoustic branch is shown in Fig. 5d and its shape agrees with the measured data, at least qualitatively. At very small $q_{||}$-values, the membranes behave as 2D liquid films and their dynamics are basically determined by the viscosity of the water layer found in between the stacked membranes (film regime). With increasing $q_{||}$ there is a transition into the bulk-elasticity regime, where the dynamics depend on the bilayer's elastic properties. At this point, the dispersion relation bifurcates in two relaxation branches (Fig. 5d). The faster of the two branches, which is beyond the experimentally accessible time window of the spin-echo spectrometer, is mainly determined by B. The slower branch can be assigned to the bending modulus K_C. The additional slow dispersion branches in Fig. 5a and b with relaxation rates of approximately 100 ns can be attributed to a surface relaxation mode (Bary-Soroker and Diamant, 2006, 2007), which is inherent to stacked membranes on a substrate (Fig. 5e).

Following the notion of Ribotta et al. (1974), the relaxation rates of bilayer undulations can be described by:

$$\tau^{-1}(q_{||}) = \frac{K_C/d}{\eta_3} q_{||}^2 \frac{q_{||}^4 + (\pi/\Lambda D)^2}{q_{||}^4 + (\pi/D)^2/\mu\eta_3} \tag{3}$$

where η_3 is the layer sliding viscosity. Using this formulation the following results were obtained for DMPC at 30 °C: $K_C = 14.8\ k_BT$; $\Lambda = 10.3$ Å; $\eta_3 = 0.016$ Pa s. K_C is well within the 7–32 k_BT range reported by different techniques (Rappolt and Pabst, 2008). B was calculated to be 2.0×10^{15} J/m^4 ($d = 54$ Å), which compares well with the range of B's ($1.0–2.2 \times 10^{15}$ J/m^4) reported by Chu et al. (2005) for DMPC at various bilayer separations. The resulting effective sliding viscosity of the membrane system η_3 was found to be 16 times higher than that of water, which points to different properties of the interstitial hydration water, compared to bulk water. Equation (3) does not describe a pure undulation mode, which is only probed at q_z values of $q_z = 2\pi/d$. If the scattering is probed at finite components $\Delta q_z = (q_z - 2\pi/d)$ or measured with coarse q_z resolution, there is a mixing with baroclinic modes, which are distinctly slower than pure bilayer undulations as they involve a relocation motion of the water layer. The parameter D describes an effective finite size cut off length, which is related to the instrumental resolution $D = \pi/\Delta q_z$.

From the soft mode present in the fluid dispersion curve at 22 °C, it seems that the phospholipid membrane is softening upon approaching T_M from the fluid phase, i.e. the regime of critical swelling or anomalous swelling (Mason et al., 2001; Pabst et al., 2003), and in agreement with results from X-ray diffraction (see above). The softening occurs at a well-defined length scale (i.e. at $2\pi/q_{||} \sim 420$ Å). While inelastic data are important to validate theoretical models and can give additional length scale information, a routine determination of membrane material parameters using spin-echo remains a challenge because of the extended acquisition times necessary in order to obtain good quality data.

Table 1
Comparison of bending (K_C) and compression (B) moduli for DMPC bilayers at 30 °C.

	Diffuse X-ray scattering from aligned bilayers[a]	X-ray scattering from vesicles[b]	Micropipette pressurization of giant bilayer vesicles[c]	Inelastic neutron scattering from aligned bilayers[d]
K_C (J)	6.9×10^{-20}	8.0×10^{-20}	5.6×10^{-20}	6.1×10^{-20}
B (J/m^4)	1.5×10^{15}	1×10^{15}	–	2×10^{15}

[a] Chu et al. (2005).
[b] Petrache et al. (1998).
[c] Rawicz et al. (2000).
[d] Rheinstädter et al. (2006a).

Table 1 compares the elastic parameters for DMPC at $T = 30$ °C as determined by the different scattering techniques discussed in this section. For the most part, the results are consistent with those found in the literature (e.g. Rappolt and Pabst, 2008 for a list of K_C values and their associated references).

4. Determining the forces between membranes

Cellular adhesion or fusion brings membranes into close contact. However, a range of complex repulsive and attractive forces are at play when such a situation arises. At large distances, repulsive electrostatic or bending fluctuation forces (Helfrich, 1973) are balanced by attractive van der Waals interactions (Parsegian, 2006). As the distance between bilayers decreases, repulsive hydration forces, whose microscopic origin may either lie in the disruption of the water's hydrogen bonded structure at the lipid/water interface (Israelachvili and Wennerstroem, 1990) or the protrusion of lipid molecules (Parsegian and Rand, 1991), come into play. Finally, steric interactions dominate when the membranes are pushed into contact, the result of lipid headgroups from apposing lipid bilayers interacting with each other (McIntosh et al., 1987).

The most prominent techniques that are applied to measuring the forces between membranes are the surface force apparatus (SFA), where single lipid bilayers are immobilized on crossed cylindrical surfaces (Israelachvili and Adams, 1978), and X-ray (McIntosh and Simon, 1986; Tristram-Nagle et al., 1998) or neutron diffraction (Pabst et al., 2002) in combination with osmotic stress. Osmotic stress (OS) may be generated either by using aqueous solutions containing large neutral polymers, such as polyethylene glycol or dextran, or by equilibrating the system in a controlled relative humidity atmosphere (Parsegian et al., 1986) (Fig. 6). Compared to SFA, the advantage of the OS technique is that the forces due to bending fluctuations are also accessible. In addition, the OS technique equally applies to MLV and aligned multibilayer samples. Because of the spatial resolution provided by scattering experiments, it is also possible to determine the forces in phase-separated systems, i.e. interacting lipid domains as demonstrated most recently by Pabst et al. (2009).

In brief, the applied osmotic pressure balances the sum of the disjoining pressures

$$\Pi = P_{vdw} + P_{el} + P_{hyd} + P_{ster} + P_{fl}, \tag{4}$$

where P_{vdw} is the van der Waals pressure, P_{el} the electrostatic pressure, P_{hyd} the hydration pressure (Marčelja and Radić, 1976), P_{ster} the steric force pressure (McIntosh et al., 1987), and P_{fl} the fluctuation force pressure (Harbich and Helfrich, 1984; Evans and Parsegian, 1986). For neutral systems (i.e. $P_{el} = 0$) and small osmotic pressures (i.e. $\Pi < 20$ atm), $P_{ster} = 0$. In this case, the only pressures that need to be considered are the van der Waals

$$P_{vdw} = -\frac{H}{6\pi}\left[d_W^{-3} - 2(d_W + d_B)^{-3} + (d_W + 2d_B)^{-3}\right], \tag{5}$$

Author's personal copy

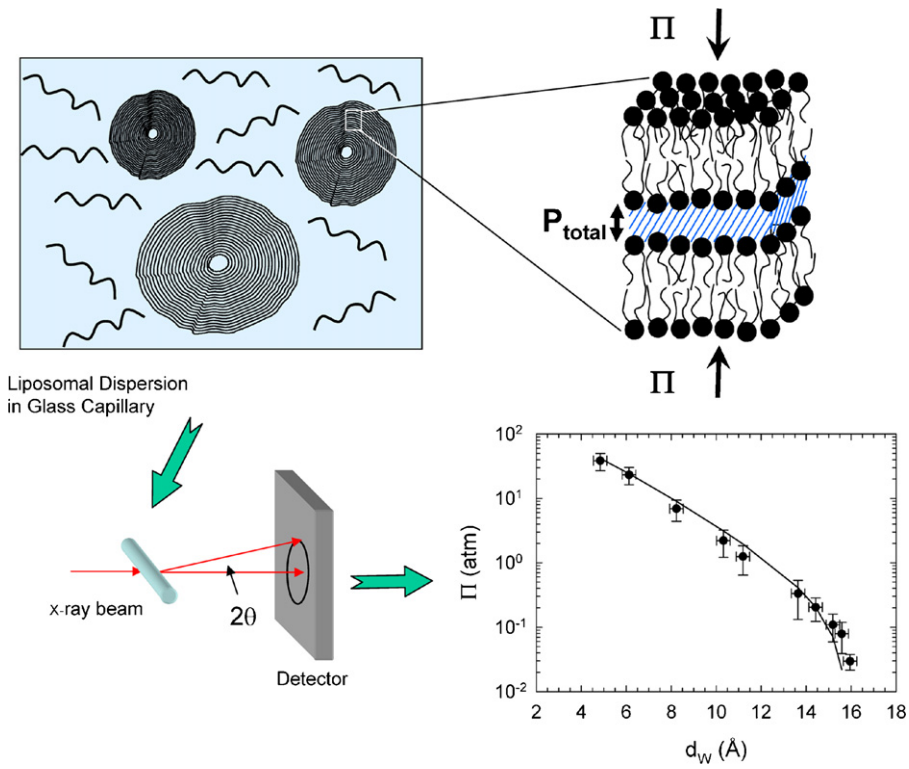

Fig. 6. Schematic of an OS experiment. The liposomal mixture is hydrated in a solution containing large molecular weight neutral polymers. The resulting osmotic pressure Π depends on the polymer type and its concentration. Π is balanced by a disjoining pressure P_{total} that depends on the sum of the interactions. The pressure isotherms, i.e. Π as a function of bilayer separation, are determined using X-ray diffraction. Experimental data are fitted using Eq. (4). The present example shows the isotherm for DOPC bilayers at 25 °C (adapted from Pabst et al., 2007a).

hydration

$$P_{hyd} = P_h \exp\left(-\frac{d_W}{\lambda_h}\right), \tag{6}$$

and bending fluctuations (Podgornik and Parsegian, 1992)

$$P_{fl} = \frac{\pi k_B T}{32\lambda_h}\sqrt{\frac{P_h}{K_C\lambda_h}}\exp\left(-\frac{d_W}{2\lambda_h}\right), \tag{7}$$

where H is the Hamaker constant, d_W the bilayer separation, d_B the membrane thickness, P_h is a scaling constant, λ_h the decay length of the hydration interactions, and k_B the Boltzmann's constant. An alternative form has been proposed for the fluctuation interactions (Petrache et al., 1998)

$$P_{fl} = \left(\frac{k_B T}{2\pi}\right)^2 \frac{A_{fl}}{K_C\lambda_{fl}}\exp\left(-\frac{d_W}{\lambda_{fl}}\right), \tag{8}$$

where the constants A_{fl} and λ_{fl} are derived from the osmotic pressure dependence of the line-shape parameter η (Eq. (1)) through high-resolution X-ray diffraction experiments.

It is clear, therefore, that even for neutral multibilayer systems, there are a number of parameters that need to be determined from pressure isotherms. Membrane thickness and bilayer separation are derived from the scattering length density profiles. Fortunately, d_B remains essentially constant up to osmotic pressures of ~20 atm. Thus, d_W can be inferred directly from the lamellar repeat distance once d_B is known for a given Π. The constants P_h and λ_h are best determined at intermediate osmotic pressures (i.e. in the approximate range of 10–20 atm), which is where the hydration force dominates the repulsive interactions, and the applied Π modulates the attractive interactions. van der Waals interaction and fluctuation forces are prominent at low Π's, and there are basically two strategies used to elucidate them. One is to fix the Hamaker constant and fit for the bending rigidity (Pabst et al., 2007a, 2009), while the other is to input K_C (determined from a separate experiment), thus obtaining H (Petrache et al., 2006a; Pan et al., 2008a, 2009). Both approaches have been successfully applied.

Another interesting aspect regarding the forces between lipid bilayers is the effect of temperature on bending fluctuations. Since bending fluctuations generally increase with increasing temperature (Eq. (1), see also Pabst et al., 2003; Mills et al., 2008; Pan et al., 2008b), the corresponding repulsive term may, at some critical temperature, overcome the attractive interactions. In this case the bilayer separation between adjacent membranes becomes ill defined and the system undergoes a critical unbinding transition, previously predicted by Lipowsky and Leibler (1986). In 2003 experimental proof for the existence of such a transition was demonstrated using a mixture of POPE/POPG (Pozo-Navas et al., 2003). X-ray data presented in Fig. 7 clearly shows the sensitivity of the technique to detect such physical phenomena.

5. Membrane structure

Biological function is intrinsically linked to membrane structure. It is believed that the structural blueprint of biological membranes is fluid phase lipid bilayers, which exhibit almost liquid-like conformational degrees of freedom so that their structure is best described by broad statistical distributions rather than sharp delta functions typical of 3D crystals. Due to this inherent disorder – which is thought to be important for proper biological function – averaged structural information is not easily obtainable, especially when said membranes are in the biologically relevant fully hydrated state. However, in recent years new approaches have been developed that take advantage of the diffuse scattering produced by undulating bilayers (see Section 3) in the disordered liquid crystalline state (Pabst et al., 2000; Lyatskaya et al., 2001; Salditt et al., 2003).

Author's personal copy

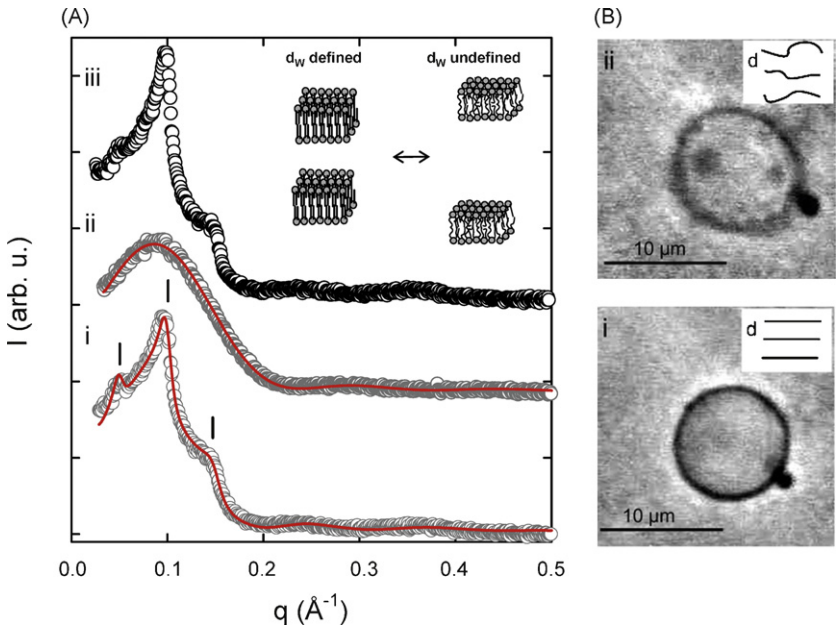

Fig. 7. Thermal unbinding of a POPE/POPG mixture due to a decrease in bilayer bending rigidity upon heating through the main phase transition T_M. a) SAX diffraction patterns from bilayers in the gel phase (bound state) exhibit Bragg peaks (indicated by dashes) (i, iii) as a result of the bilayers being positionally correlated over an extended distance. Upon entering the fluid phase, the system loses these long-range correlations and exhibits pure diffuse scattering (ii) (unbound state). Reversibility of the transition is demonstrated by cooling the sample below T_M (iii). b) Optical microscopy images of MLVs obtained in phase contrast mode show sharp (i) and fuzzy (ii) boundaries below and above the unbinding temperature, respectively (adaped from Pozo-Navas et al., 2003, 2005).

5.1. Single component membranes

A parameter needed to accurately describe bilayer structure, and lipid–lipid and lipid–protein interactions in biomembranes is a lipid's lateral area, A (for a compendium of lipid areas please see Rand and Parsegian, 1989; Nagle and Tristram-Nagle, 2000). In addition to playing a key role in describing membrane structure, knowledge of A is central to simulations (Klauda et al., 2006). However, despite their central role in membrane biophysics, the values of lipid lateral areas have been, to some extent, controversial. Although the largest discrepancies have been resolved, significant discrepancies still remain when comparing lipid areas as determined from X-ray and neutron scattering experiments.

For both X-ray and neutron scattering A is calculated using the bilayer's thickness and volumetric information. However, the two techniques are sensitive to different bilayer thicknesses. The thickness best resolved by X-rays is the distance between the lipid headgroup phosphates D_{HH}. As a result, assumptions are made in order to obtain the hydrocarbon chain thickness D_C and total bilayer thickness (hydrocarbon chains plus headgroups) D_B. On the other hand, in neutron scattering the high contrast between the protonated lipid and deuterated water accurately defines this structural feature (i.e. D_B) and A can be directly obtained using the precisely measured lipid volume. Despite this advantage, due to the scarcity of neutron data A has almost exclusively been determined using X-rays.

The joint refinement of X-ray and neutron diffraction data to obtain bilayer structural information was first reported by Wiener and White (1991a). Even though they used highly ordered, partially dehydrated multibilayers, those experiments illustrated the challenges faced by the diffraction method when it came to studying aligned stacks of bilayers. Recently, however, a similar approach for calculating scattering density profiles (SDPs) was introduced by Kučerka et al. (2008a). This new method of simultaneously analyzing X-ray and neutron small angle scattering data has resulted in decreasing the number of parameters needed to fit the data by nearly 50% compared to the original composition-space model (Wiener and White, 1991b). The analysis by Kučerka et al. utilizes the continuous diffuse scattering from aligned multibilayers, observed at mid-to-high scattering vectors q (i.e., $0.2\,\text{Å}^{-1} < q < 0.8\,\text{Å}^{-1}$), and the diffuse scattering from isotropic unilamellar vesicles (ULVs), extending the q range down to $\sim 0.05\,\text{Å}^{-1}$ (Kučerka et al., 2005). By appropriately parsing a lipid molecule (aided by molecular dynamics (MD) simulations) and simultaneously analyzing the different data, including the various contrast neutron data, the precise structure of fully hydrated, liquid crystalline bilayers could be determined (Fig. 8) (Kučerka et al., 2009b). More importantly, the new analysis indicated that areas for some lipids have been overestimated by as much as 10% (see Table 2).

This result highlights the need to revisit lipid areas as they are often used to compare with MD simulations. For example, MD simulations based on CHARMM potentials are performed at non-zero surface tension in order to obtain better agreement with X-ray scattering data (Klauda et al., 2006), while simulations using a combination of GROMOS and OPLS potentials do not seem to require this additional "tweaking" (Anezo et al., 2003). Since MD force fields are considered to be "well tuned" if they are able to reproduce experimental data (Sachs et al., 2003), more work is needed in order to reconcile simulation and experiment, even in the simplest case of single component membranes.

Table 2
Lipid structural data using the scattering density profile (SDP)[a] model analysis.

Lipid	Temp. (°C)	D_{HH} (Å)	$2D_C$ (Å)	D_B (Å)	A (Å^2)
16:0-16:0 PC (DPPC)[a]	50	38.0	28.4	39.0	63.1
18:1-18:1 PC (DOPC)[a]	30	36.7	28.8	38.7	67.4
14:1-14:1 PC[b]	30	29.6	23.4	33.7	64.2
16:1-16:1 PC[b]	30	32.1	26.2	36.2	65.8
18:1-18:1 PC[b]	30	36.8	29.0	38.9	66.9
20:1-20:1PC[b]	30	38.9	32.6	42.5	66.6
22:1-22:1 PC[b]	30	45.5	36.4	46.4	65.7
24:1-24:1 PC[b]	30	47.9	41.6	52.2	62.7

[a] Kučerka et al. (2008a).
[b] Kučerka et al. (2009b).

Author's personal copy

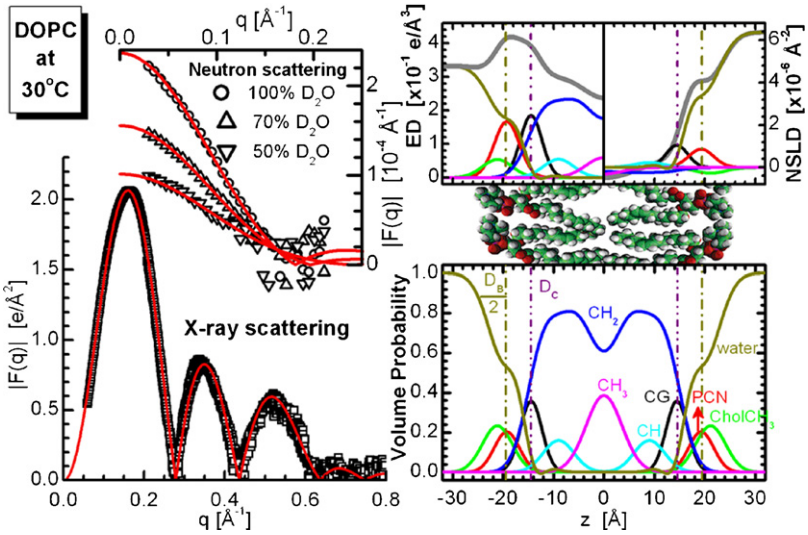

Fig. 8. Illustration of lipid bilayer structure determination by the simultaneous analysis of X-ray and neutron scattering data. Graphs on the left hand side show the experimentally determined X-ray and contrast varied neutron scattering form factors (points), together with the best fits (red lines) to the data. Right hand side panels show the SDP model representation of a bilayer in real space (depicted by the schematic in the centre). The top panel shows electron densities (ED) (left) and neutron scattering length densities (NSLD) (right) of the various lipid component distributions, including the total scattering density (thick gray lines). The bottom panel shows volume probability distributions, where the total probability is equal to 1 at each point across the bilayer. Figure was adapted from Kučerka et al. (2008a) and Kučerka et al. (2009b).(For interpretation of the references to color in this figure, the reader is referred to the web version of the article.)

5.2. Lipid mixtures and domains

In general, the thermodynamic behaviour of lipids falls into three broad categories: (i) ideal mixing, where phase separation does not take place; (ii) non-ideal or non-random mixing, where compositional fluctuations take place but no stable domains are formed; and (iii) macroscopic phase separation, where micron-size stable lipid domains are formed. Cases (i) and (ii) occur most frequently in binary lipid mixtures, whereas large stable domains have only been reported in ternary lipid mixtures (e.g. Baumgart et al., 2003; Veatch et al., 2004). For the most part, diffraction techniques are not capable of distinguishing between cases (i) and (ii) as the fluctuating "domains" formed in (ii) occur on timescales much faster (on the order of ms to ns) than the experiment, which is usually of the order of seconds to minutes. An example of such behaviour is found in binary cholesterol–PC mixtures.

Several spectroscopic techniques have detected a fluid–fluid phase coexistence regime of the so-called liquid disordered (*ld*) and liquid ordered (*lo*) phases – Ipsen et al. (1987) and Vist and Davis (1990) were the first to report this. In turn scattering experiments always reported a uniform bilayer, with no indications of phase separation (Hodzic et al., 2008; Mills et al., 2009) (Fig. 9). As such, these examples illustrate the ongoing debate of whether or not functional domains exist in biological systems.

In the case of macroscopic phase separation, lipid domains in multilamellar assemblies interestingly form large scattering domains that are in registry with one another (e.g. Karmakar et al., 2006). Thus, the Bragg peaks as a result of the coexisting lamel-

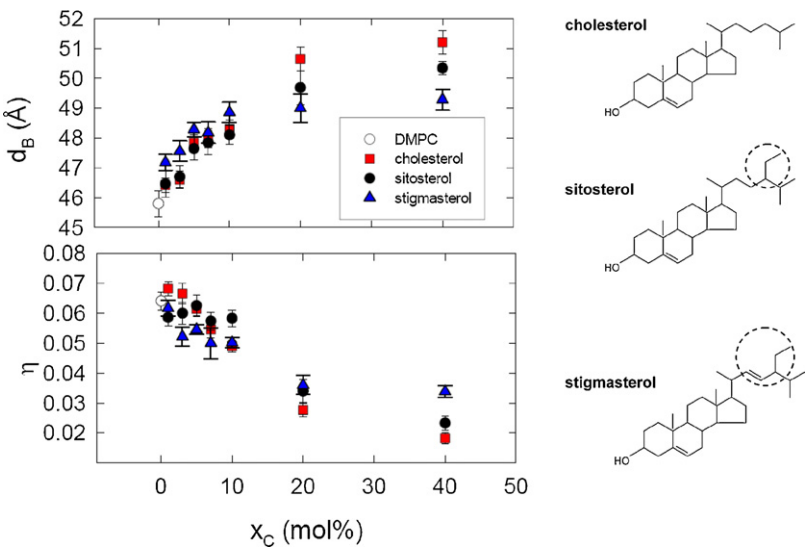

Fig. 9. Membrane thickness d_B and the fluctuation parameter η plotted as a function of cholesterol, sitosterol and stigmasterol concentration in DMPC bilayers at 35 °C. No signature of phase separation is observed and the bilayers appear as a uniform phase. An increase in membrane thickness and a decrease in bending fluctuations are the result of the membrane condensing effect by sterols. Although the two plant sterols differ marginally from cholesterol in their chemical structure (see encircled regions), they exhibit a weaker condensing effect, demonstrating the importance of chemical composition. Data from Hodzic et al. (2008).

Author's personal copy

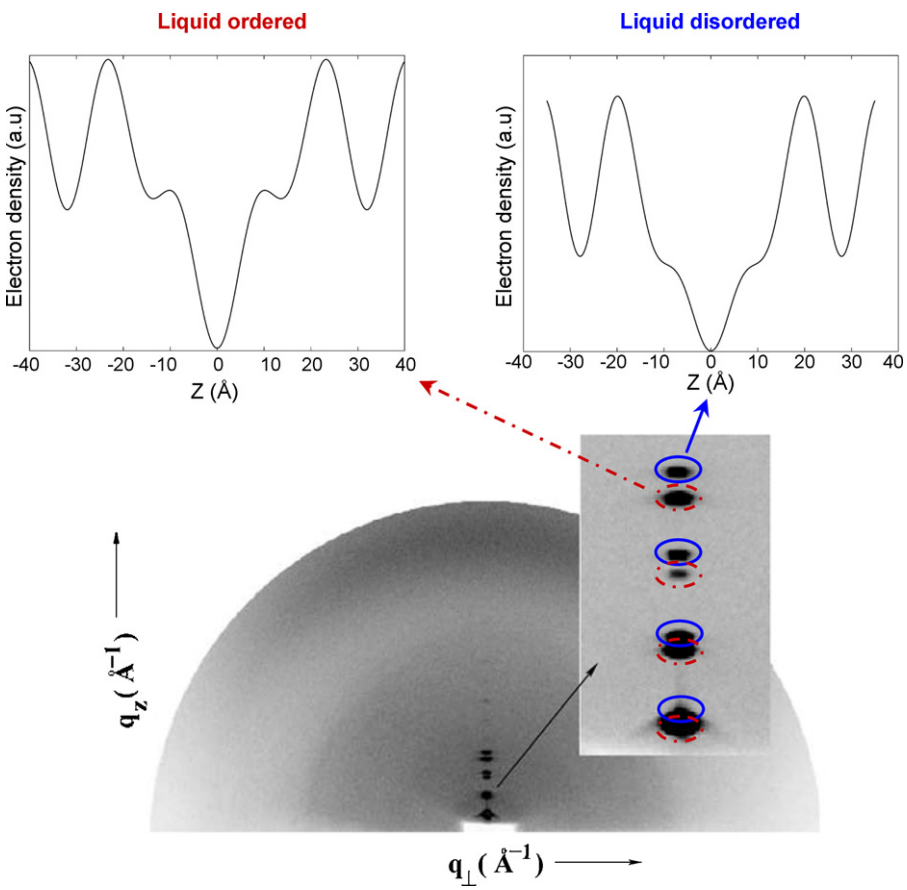

Fig. 10. 1D EDPs and diffraction pattern of an aligned DPPC/DOPC/cholesterol mixture clearly showing the presence of two lamellar phases that are attributable to the *lo* and *ld* phase (adapted from Karmakar et al., 2006).

lar phases can be well separated, individually analysed, and their 1D EDPs determined (Fig. 10).

Diffraction techniques are also capable of probing the supramolecular properties of membranes, for example the thickness of lipid domains (Gandhavadi et al., 2002) and the distribution of cholesterol in bilayers leaflets (Kučerka et al., 2009c). Recently, the coexistence of tilted and interdigitated lamellar phases was observed in anionic bilayers composed of distearoyl PG (DSPG, 18:0-18:0 PG) (Pabst et al., 2007b), and asymmetric bilayers were observed in the case of the charged lipid dioleoyl phospatidylserine (DOPS, 18:1-18:1 PS) (Kučerka et al., 2007). Although it is not entirely clear why single component bilayers exhibit heterogeneous structures, these examples point to the fact that domains can be distinguished from the diffuse X-ray scattering of homogeneous ULVs through the appropriate data analysis (Fig. 11).

Recently, OS measurements were performed on a lipid mixture of sphingomyelin (SM), POPC and ceramide, a mixture which exhibits a fluid-gel phase coexistence at a particular ceramide concentration (Pabst et al., 2009). It was determined that the bending rigidity of the fluid phase of the SM/POPC/ceramide mixture (that coexists with the gel phase) is much smaller than the fluid phase of the SM/POPC mixture. This unintuitive result can be understood in terms of SM depleted fluid domains as a result of SM's preferred interaction with ceramide.

Additionally, neutron scattering in combination with contrast variation is also able to probe the average size and form of coexisting domains on unilamellar vesicles (ULVs). While the idea of using small angle scattering (SAS) to characterize membrane lateral heterogeneities is not new, there have been few such studies. It is only in the recent past that the methodology has been developed for the detection and characterization of domains in laterally heterogeneous ULVs via SANS (Pencer et al., 2005, 2006, 2007; Anghel et al., 2007). It was shown that through the appropriate use of selective deuteration, neutrons are capable of probing and characterizing lateral heterogeneities in model membrane systems, both qualitatively and quantitatively.

As mentioned, there is ongoing controversy regarding the size and stability of membrane domains in both cell and model membranes. This controversy is further complicated by the variability in sensitivity among the different techniques used to detect

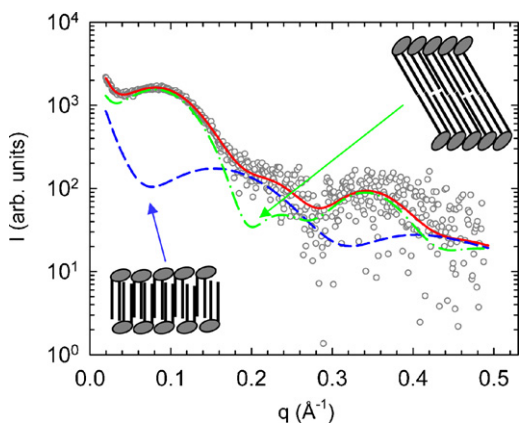

Fig. 11. Small angle X-ray scattering (SAXS) pattern of DSPG bilayers at 45 °C. Due to the membrane's net negative surface charge, the system displays no sharp Bragg peaks, but diffuse scattering originating from single bilayers. A global fit (i.e. over the entire *q* range) to the data distinguishes two features, namely interdigitated and tilted non-interdigitated phases (figure adapted from Pabst et al., 2007b).

Author's personal copy

domains, and by the number of model membrane systems studied. In particular, the observation of lateral heterogeneities in ULVs by fluorescence resonance energy transfer (FRET), where none are observed in giant unilamellar vesicles (GUVs) by fluorescence microscopy (FM), has led to fundamental questions regarding the nature and existence of membrane domains (Feigenson and Buboltz, 2001). The recently developed SANS approach for studying lateral membrane heterogeneities has helped to reconcile these apparent discrepancies. It was discovered that membrane curvature has a significant role to play in the miscibility of the various lipid components (Pencer et al., 2008). Specifically, that increased membrane curvature (decreased ULV size) induces lipid demixing. It therefore seems that the apparent inconsistencies between ULV FRET and GUV FM studies may simply be explained by differences in membrane curvature.

5.3. "Bicelle" mixtures: resultant morphologies

In addition to lateral domains and bilayer asymmetry, lipid mixtures also aggregate into morphologies that offer biophysists new capabilities. One such example is the well-known "bicelle" lipid mixture, which is generally made up of a combination of long-chain and short-chain phospholipids. As some morphologies formed by bicelle lipid mixtures (Fig. 12) are magnetically alignable, NMR spectroscopists have used these mixtures to incorporate and magnetically align membrane associated proteins in their functional states (e.g. Sanders and Schwonek, 1992; Sanders and Landis, 1995; Vold et al., 1997; Prosser et al., 1998a,b; Losonczi and Prestegard, 1998; Whiles et al., 2002).

The structure of the magnetically alignable phase formed by bicelle mixtures was initially proposed as being comprised of bilayered disks (Fig. 12a) – as deduced from early NMR data – where the long-chain lipids formed the planar portion of the disk and the short-chain lipids segregated into the disk's rim (Sanders and Landis, 1995; Raffard et al., 2000; Sternin et al., 2001). Although NMR is a powerful technique for probing the molecular local environment, SANS and SAXS techniques are capable of determining the aggregate morphologies. For example, the structural phase diagram of Tm^{3+}-doped bicelle mixtures – as determined by SANS – revealed that the magnetically alignable morphology was in fact perforated

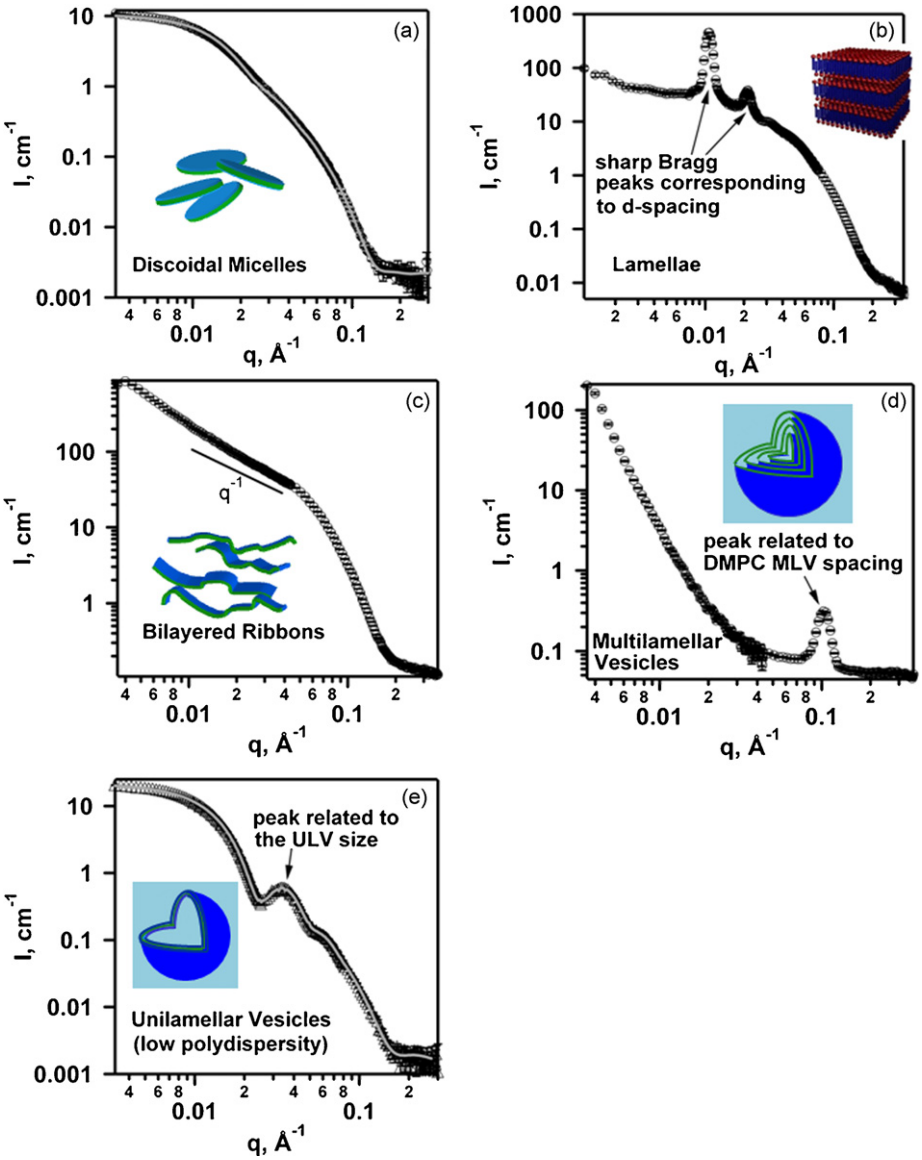

Fig. 12. SANS patterns from the various morphologies (insets) formed by "bicelle" lipid mixtures: a) bilayered disks; b) low-polydispersity ULVs; c) lamellae with a well-defined repeat spacing; d) bilayered ribbons, where $I(q) \sim q^{-1}$; and e) DMPC MLVs with a characteristic d-spacing of ~62 Å. The grey curves in a) and b) are best fits to the SANS data using the models shown in the insets to the figures.

Author's personal copy

lamellae (Fig. 12b), not bilayered disks as previously implied by NMR (Nieh et al., 2001, 2002). The high curvature edges of the perforations are stabilized by the short-chain phospholipids. The presence of a lamellar phase was based on the fact that sharp Bragg peaks were observed, as well as the bilayer repeat spacing increasing in a 1D manner with elevated levels of hydration (Fig. 12b). The high viscosity (Hwang and Oweimreen, 2003) and high degree of alignment observed under magnetic fields and shear flow (Nieh et al., 2003) are also consistent with the proposed morphology.

Later SANS studies of bicelle lipid mixtures indicated that charge density also plays an important role in the resultant morphologies. For example, bilayered ribbons (Fig. 12c) and perforated lamellae were found in neutral and charged systems, respectively (Nieh et al., 2004; Harroun et al., 2005; Katsaras et al., 2005). The ribbons transformed into MLVs with increasing temperature, while the charged perforated lamellae remained unaltered. In the case of high total lipid concentration (≥20 wt.%) systems, the lamellar phase is comprised of entangled ribbons, as was recently confirmed using a combination of SANS and pulsed field gradient NMR studies (Soong et al., 2010). It should be pointed out that bilayered disks were identified by SANS to exist at low temperature (Harroun et al., 2005), where the NMR signal was found to be isotropic. Moreover, the high temperature phases, which are not always magnetically alignable, have been shown to contain either MLVs (Fig. 12d) or ULVs (Fig. 12e), depending on the total lipid concentrations and charge density (Nieh et al., 2005a,b; Katsaras et al., 2005). The size of these ULVs is, for the most part uniform, but strongly depends on their path of formation (Mahabir et al., in press). Moreover, these uniform size ULVs are capable of encapsulating materials and releasing them in a controlled fashion (Nieh et al., 2008). Most recently, such ULVs have been tested as carriers for magnetic resonance imaging contrast agents, further evidence of their potential with regards to biomedical applications (Nieh et al., 2009). Of note, is that many of the aforementioned morphologies have also been confirmed by cryo-transmission electron microscopy (cryo-TEM) (e.g. Van Dam et al., 2004, 2006).

6. Membrane active compounds

Phospholipid membranes are highly susceptible to lipophilic, hydrophilic and amphiphilic substances that incorporate into the bilayer's interior or adsorb to the lipid/water interface. The interactions of such compounds with lipid membranes may thus be probed using the membrane's structural features as highly sensitive reporters of changes to a membrane's properties. It should be noted, however, that usually the best strategy is not to focus on a single membrane property, such as for example membrane thickness, but to monitor several membrane parameters simultaneously.

6.1. Effect of peptides on bilayer properties

In the last decade, lipid–protein interactions have become a central focus of much research. For example, proteins featuring transmembrane domains (e.g. ion channels) lead to a local elastic deformation of the membrane according to the principle of hydrophobic matching (Killian, 2003), which leads to the formation of selective lipid domains. Likewise lipids may be involved in sorting proteins into domains (i.e. rafts) (Simons and van Meer, 1988; Simons and Vaz, 2004), or affect the conformational equilibrium of proteins, and hence their function, for example through depth-dependent changes of the lateral pressure profile (Cantor, 1997).

Transmembrane protein domains are typically made up of α-helices. Hence, the effects of integral proteins on lipid membranes can, to a first approximation, be studied using α-helical peptides.

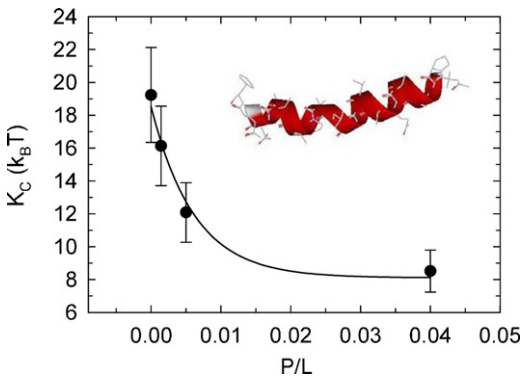

Fig. 13. The bending rigidity of DOPC bilayers as a function of alamethicin concentration. At low peptide-to-lipid (P/L) ratios, alamethicin adsorbs to the membrane. It then subsequently inserts and forms barrel-stave pores at high P/L ratios. During this insertion process the membrane experiences a softening effect. Data taken from Pabst et al. (2007a), and inset shows the crystallographic structure of alamethicin (Fox and Richards, 1982).

Alamethicin is a 20 amino acid fungal peptide from *Trichoderma viride* and is known to form pores in membranes (Bezrukov and Vodyanoy, 1997). This pore formation ability is promoted by its amphiphatic α-helical structure, where the peptide's hydrophobic side faces the membrane's interior and its hydrophilic side forms the aqueous surface of the pore. At very low peptide-to-lipid molar ratios, alamethicin, like many other amphiphatic peptides, adsorbs to the membrane with its helical axis parallel to the membrane surface, leading to a local deformation (He et al., 1996; Heller et al., 1997). As the peptide concentration is increased, the peptides accumulate on the membrane surface – possibly aggregating – and above a certain threshold concentration insert transversally into the membrane forming a pore (Huang, 2006). Using the OS technique in combination with X-ray scattering, it was shown by Pabst et al. (2007a) (Fig. 13) and later on by Pan et al. (2009) that the pore formation process "softens" DOPC bilayers by ~50%. This result is consistent with the other studies that recorded a drop in membrane bending rigidity in the presence of amphiphatic peptides (Vitkova et al., 2006; Tristram-Nagle and Nagle, 2007).

Pore formation by amphiphatic peptides has also been associated with bilayer thinning as a result of local deformation at low peptide concentrations and hydrophobic matching at high peptide concentrations (Lee et al., 2004). However, the system allows for more degrees of freedom. Most recently, Pabst et al. (2008) reported membrane thickening in the case of the antimicrobial peptide peptidyl-glycylleucine-carboxylamide (PGLa) in anionic bilayers composed of phosphatidylglycerol. This observation can also be rationalized in terms of hydrophobic matching, which causes the membrane to thicken if the hydrophobic length of the peptide is larger than d_B. Furthermore, if the mismatch is too great, then the peptide may tilt within the membrane's interior such that it's projected length better matches d_B. However, if both the hydrophobic length of the peptide and the membrane thickness match ideally, no changes to the membrane thickness may be detected. Hence, membrane thinning is not a unique signal for peptide pore formation and consequently, d_B is not the ideal parameter for making this determination.

6.2. Ion-specific effects

In addition to lipid–protein interactions, the significance of the aqueous phase for the proper functioning of biological membranes cannot be overestimated. Biological membranes are surrounded by an electrolytic liquid containing Na^+, K^+, Ca^{2+}, Mg^{2+} or Cl^- ions.

Author's personal copy

Their interactions with cell membranes are understood to influence, for example the gating of ion channels, membrane fusion and membrane "fluidity" (see Section 3). Over the years, there have been copious amounts of biophysical reports demonstrating that ions affect the physical properties of lipid bilayers (Lis et al., 1980, 1981; Loosely-Millman et al., 1982). For example, ions influence the average lipid head group tilt angle (Seelig et al., 1987) and may even lead to lipid aggregation (Böckmann et al., 2003). The observed effects depend, however, on ion size, valency and polarizability following the phenomenological Hofmeister series – a classification of ions categorized by their ability to alter the structure of water (Kunz et al., 2004).

Monovalent ions weakly adsorb to the surface of neutral bilayers and can lead to concentration dependent swelling in multibilayer systems. This can be understood in terms of the effect that ions have on the membrane's interacting forces. Due to the binding of ions, additional electrostatic interactions arise which are partially screened by the diffuse double layer of counter-ions. Additionally, low frequency charge fluctuations decrease with increasing concentration of ions leading to an effective decrease of the van der Waals attraction. Furthermore, the ions compete with the interfacial lipid headgroup water leading to the formation of a salt exclusion layer (Petrache et al., 2005, 2006b). In POPC, for example, it has been shown that Na^+ causes a significant rigidification of the bilayers at high salt concentration (Pabst et al., 2007c).

The swelling behaviour induced by divalent salts in neutral lipid bilayers is even more complicated. Due to their (i.e. salts) much higher affinity for neutral membranes, the bilayers become exceedingly charged, even at low salt concentrations, leading to a complete loss of positional correlation between multibilayers (Inoko et al., 1975; Yamada et al., 2005). As the Ca^{2+} ion concentration increases, screening by the counterions in solution comes in to play, and bilayer separation decreases (not the case of Na^+). At this point, the water spacing is even smaller than in bilayers in the absence of ions, including Na^+, indicating that adjacent bilayers are somehow attracted to each other. However, a further increase in Ca^{2+} concentration causes d_W to increase. (Pabst et al., 2007c) (Fig. 14). This increase in d_W is most likely due to an decrease in the van der Waals attraction force, as was the case with monovalent cations. The attraction at intermediate salt concentrations exhibited by these bilayers is presently not understood. Nevertheless, like in the case of monovalent Na^+ ions, the presence of the divalent Ca^{2+} cation leads to increased membrane stiffness at high salt concentrations (Pabst et al., 2007c).

The effect of Ca^{2+} cations was recently reported in membranes composed of lipopolysaccharides (LPS). Small angle neutron diffraction data showed that water penetrates Ca^{2+}-LPS bilayers to a lesser extent than either Mg^{2+}-LPS or Na^+-LPS bilayers (Kučerka et al., 2008b). While Ca^{2+} cations make LPS bilayers more compact and less permeable to water, a significant amount of water was found to penetrate deep into Mg^{2+}-LPS and Na^+-LPS bilayers, including the bilayer's hydrophobic center. It is believed that such increased levels of hydration could be associated with enhanced biological activity in these bacterial membranes. As such, a more accurate determination of the membrane's structure may allow for a better understanding of membrane function. For example, differences in a bilayer's permeability to water could have implications with regards to how small molecules permeate through the outer membrane of Gram-negative bacteria, and may aid in the development of more effective antibiotics.

7. Membrane dynamics

Motions in proteins and membranes take place on various length and time scales (Frauenfelder et al., 1991; Fenimore et al., 2004). The proper functioning of membrane proteins most likely depends on membrane composition and physical properties, such as its elastic properties (see Sections 3 and 4) and hydrophobic thickness (see Section 5). Dynamic processes in complex biological membranes also involve interactions between the membrane's different constituents, such as lipids, cholesterol, proteins, etc. (Rheinstädter et al., 2008a; Rheinstädter et al., 2009).

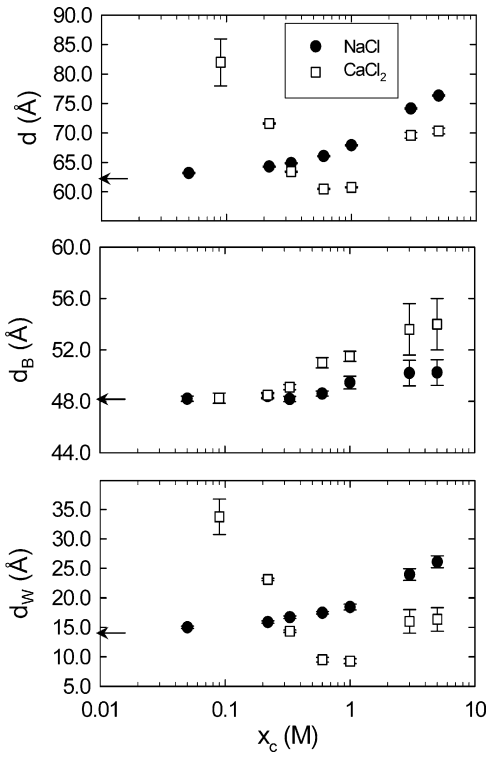

Fig. 14. Lamellar repeat distance d, bilayer thickness d_B and water thickness d_W exhibited by POPC multibilayers at 27 °C, as a function of NaCl and $CaCl_2$ concentration. The increase in d_B observed in the presence of high ion concentration is more pronounced for the divalent Ca^{2+} ion, and can be understood in terms of membrane stiffening. The effect on membrane swelling behaviour is markedly different between the two ion species, the result of differing binding affinities and valencies, both of which affect interbilayer forces (adapted from Pabst et al., 2007c).

Biologically relevant materials can be thought of as "multi-scale" materials, due to their relevant dynamics taking place over extended length and time scales. To address this multi-scale behaviour experimentally, different techniques must be applied. Fig. 15 depicts the length and time scales accessible by inelastic X-ray, inelastic neutron, DLS, Brillouin and Raman scattering, and dielectric spectroscopy. By combining the different techniques a large range of dynamical behaviour can be elucidated. For example, inelastic neutron and X-ray scattering access length scales from less than 1 Å to greater than 100 nm, and time scales from picoseconds to almost 1 ms (Fig. 15). While inelastic X-ray scattering is the perfect tool to measure fast dynamics at large distances (i.e. small q), inelastic neutron scattering can more easily and precisely access slow dynamics at smaller length scales (large q). In recent years, MD simulations are also proving to be an invaluable tool in developing models for molecular structure and dynamics in membranes and proteins. Because of the ever-increasing computing power and optimized algorithms, large complex systems (i.e. many hundreds of molecules) and long simulation times can now be addressed (e.g. Smith, 1991; Tarek et al., 2001; Tarek and Tobias, 2002; Hayward and Smith, 2002; Wood et al., 2007; Meinhold et al., 2007; Marrink et al., 2007). The dashed rectangle in Fig. 15 marks the dynamic range currently accessed by computer simulations – the elementary time scale for simulations is in the order of femtoseconds.

Author's personal copy

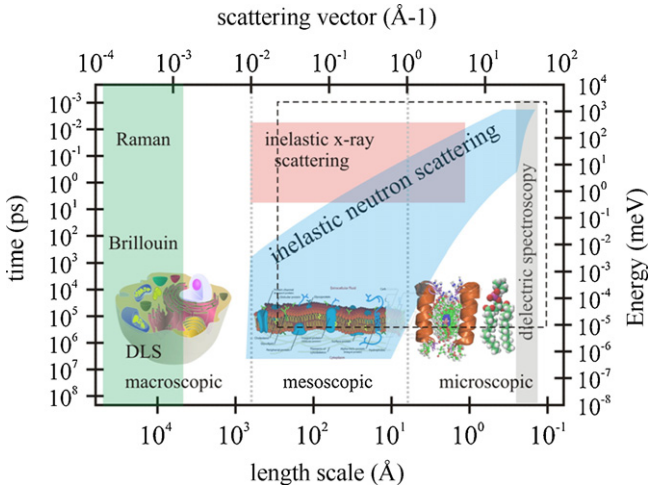

Fig. 15. Length and time scales, and corresponding energy and momentum transfers, for spectroscopic techniques covering a range of dynamics from the microscopic to the macroscopic. Light scattering techniques include Raman, Brillouin, and dynamic light scattering (DLS). Inelastic X-ray and neutron scattering access dynamics on Å and nm length scales. Dielectric spectroscopy probes the length scale of an elementary molecular electric dipole, which can be estimated through the C–O bond length (~140 pm). The area within the dashed line box is the dynamical range accessible by computer simulations.

7.1. Inelastic neutron scattering

Motions in lipid bilayers range from long wavelength undulation and bending modes, with typical relaxation times on the order of nanoseconds and lateral length scales of several hundred lipid molecules (i.e. tens of nanometers), to short wavelength density fluctuations in the picosecond range and nearest neighbour length scales (Pfeiffer et al., 1989, 1993; König et al., 1992, 1994, 1995; Lipowsky and Sackmann, 1995; Lindahl and Edholm, 2000; Bayerl, 2000; Salditt, 2000; Rheinstädter et al., 2004, 2005, 2006a, 2007; Rheinstädter, 2008b). Different techniques have been used to study the various types of motions. For example, local dynamics in lipid bilayers (i.e. individual lipid molecules), such as vibration, rotation, libration (hindered rotation) and diffusion, have been investigated by incoherent neutron scattering (Pfeiffer et al., 1989, 1993; König et al., 1992, 1994, 1995) and NMR (Bloom and Bayerl, 1995; Nevzorov and Brown, 1997) in order to determine the short wavelength translational and rotational diffusion constants. On the other hand, collective bilayer undulations have been examined by coherent scattering experiments using neutron spin-echo spectrometers (Pfeiffer et al., 1989, 1993; Takeda et al., 1999; Rheinstädter et al., 2006a) and DLS (Hirn et al., 1999; Hirn and Bayerl, 1999; Hildenbrand and Bayerl, 2005), while collective short wavelength dynamics have been studied by inelastic X-ray (Chen et al., 2001) and neutron (Rheinstädter et al., 2004) scattering using the ubiquitous triple-axis spectrometer invented by B.N. Brockhouse in the 1950s. In contrast to other spectroscopic techniques, for instance, dielectric spectroscopy, inelastic X-ray and neutron scattering result in wave vector resolved access to molecular dynamics. For example, excitation frequencies and relaxation rates are measured at the different internal length scales of the system. A typical dynamical scattering experiment measures (q,ω) pairs, resulting in a frequency along with a corresponding length scale, and possibly a corresponding direction (e.g. parallel or perpendicular to a protein's axis), additional information of paramount importance when it comes to relating dynamical information to structure. In short, the suite of inelastic instruments used to study soft and biologically relevant materials comprises of time-of-flight, backscattering, triple-axis and spin-echo spectrometers (Teixeira et al., 2008; Rheinstädter et al., 2006b,c).

7.2. Interactions in membranes

Understanding how proteins (biology's worker molecules) interact with each other is one of biology's ultimate goals, and at the same time, one of its greatest challenges. A possible dynamical coupling between proteins (i.e. cooperative protein dynamics) is necessary for the understanding of macromolecular function at the cellular level as it may be responsible in effective inter protein communication. The commonly assumed interaction mechanism between inclusions in membranes is that of a lipid mediated interaction, the result of local distortions within the lipid bilayer (Dan et al., 1993; Kralchevsky, 1997; Cantor, 1997; Lagüe et al., 2001; Biscari and Bisi, 2002; Bohinc et al., 2003), which are believed to be manifested, in part, through the bilayer's elastic properties.

Collective molecular motions in proteins (and also DNA) have recently created much discussion not only because of their potential impact on membrane function, but also with regards to our general understanding of biological systems. Inter protein dynamics in a carboxymyoglobin protein crystal were recently reported using an MD simulation (Meinhold et al., 2007; Kurkal-Siebert et al., 2008). Experimentally, phonon-like excitations of proteins in a hydrated protein powder sample were reported from inelastic X-ray experiments (Liu et al., 2008), and protein-protein interactions in purple membrane (PM) were reported from inelastic neutron scattering measurements (Rheinstädter et al., 2009). Due to its simple organization and easy spectroscopic access of its functional state, PM is one of the best suited model systems for the observation of collective protein dynamics.

PM occurs naturally in the form of 2D crystals consisting of 75% (wt./wt.) of the protein bacteriorhodopsin (BR) (that functions as a light activated proton pump) and 25% of a variety of lipid species, mostly phospholipids and glycolipids (Haupts et al., 1999). PM structure has been well established by electron microscopy, and neutron and X-ray diffraction experiments (e.g. Koltover et al., 1998, 1999; Haupts et al., 1999; Zaccai, 2000a,b; Neutze et al., 2002; Lanyi, 2004), and consists of seven transmembrane α helices arranged around the photosensitive retinal molecule. The protein in the lipid matrix is organized in trimers that form a highly ordered 2D hexagonal lattice, with a lattice parameter $a \sim 62$ Å. A model of the 2D protein lattice in PM is shown in Fig. 16a. The basic hexagonal translations are indicated by arrows. The interaction between protein trimers is contained within the springs with an effective (longitudinal) spring constant k. The calculated longitudinal spectrum $C_l(q,\omega)$ is defined by $C_l(q,\omega) = (\omega^2/q^2)S(q,\omega)$, and is shown in Fig. 16b. The statistical average in the plane of the membrane leads to a superposition of the different phonon branches which start and end at the hexagonal Bragg peaks (at $\hbar\omega = 0$). The data points are the excitation positions as determined from the inelastic neutron triple-axis experiment (Rheinstädter et al., 2009).

The effective protein–protein spring constant k was determined to be about 54 N/m. The amplitude of this mode of vibration can be estimated from the equi-partition theorem to $\sqrt{<x^2>} = \sqrt{k_B T/k} = 0.1$ Å, and the interaction force between two neighbouring trimers to $F = k\sqrt{<x^2>} = 0.5$ nN. For comparison, using the same approach the spring constant for graphite was calculated to be 27,000 N/m for the in-plane interaction, and 3.5 N/m for out-of-plane interactions. The protein interaction force constant for PM is therefore 1–2 orders of magnitude larger than the effective van-der-Waals force constant found in graphite, but 2–3 orders of magnitude weaker than a C–C bond. In contrast, the amplitudes of diffusive, self-correlated motions are usually about one magnitude larger than those of collective pair correlated motions (Zaccai, 2000a,b; Rheinstädter et al., 2009). From this, one can conclude that the spectrum of thermal fluctuations in a biological membrane is most likely dominated by the diffusive motions of lipids and proteins. Interactions, however, may become more relevant for certain

Author's personal copy

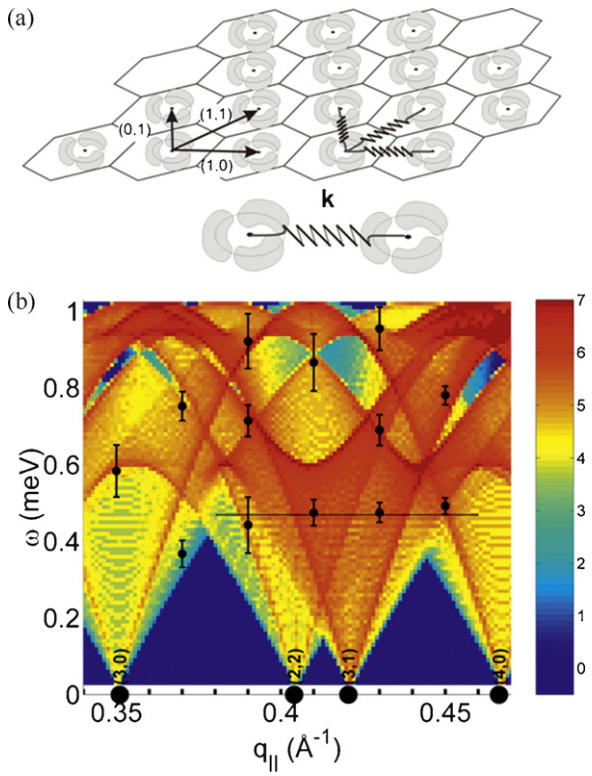

Fig. 16. a) BR trimers are arranged on a hexagonal lattice of lattice constant $a = 62$ Å. The interaction between the protein trimers is depicted as springs with effective spring constant k. b) The calculated excitation spectrum $C_1(q,\omega)$ is in the range of the experimental data. Data points mark the positions of the excitations. The horizontal line at $\hbar\omega = 0{:}45$ meV marks the position of a possible optical phonon mode, not included in the calculations (adapted from Rheinstädter et al., 2009).

functions, such as the photo cycle (Luecke et al., 1999b) and signal transmission.

8. Concluding remarks

Diffraction techniques, especially with regards to X-rays, have traditionally been used to determine the structure of 3D crystals. Over the past decades, X-ray diffraction has been used to elucidate the structure of a wide range of materials to atomic resolution – starting with common table salt in 1914. However, a few decades ago nobody could have envisioned that diffraction techniques would develop to an extent that they would successfully characterize the physical properties of disordered materials, such as biomimetic membranes. In this review we have presented some of the latest research regarding the application of X-ray and neutron scattering methods to elucidate the material properties previously thought to be the domain of other techniques (e.g. NMR and Raman spectroscopies, optical and electron micrscopies, etc.). Over the next decade, as some of the techniques discussed here and others (e.g. MD simulations, various optical microscopies, to name but a few) reach maturity, we will for the first time have unique access to the much touted structure–function relationship that is universally sought out in biology.

References

Abbott, A., 2005. Hopping fences. Nature 433, 680–683.

Akers, C.K., Parsons, D.F., 1970. X-ray diffraction of myelin membrane: II Determination of the phase angles of the frog sciatic nerve by heavy atom labeling and calculation of the electron density distribution of the membrane. Biophys. J. 10, 116–136.

Anezo, C., de Vries, A.H., Holtje, H.D., Tieleman, D.P., Marrink, S.J., 2003. Methodological issues in lipid bilayer simulations. J. Phys. Chem. B 107, 9424–9433.

Anghel, V.N.P., Kučerka, N., Pencer, J., Katsaras, J., 2007. Scattering from laterally heterogeneous vesicles II: the form factor. J Appl. Cryst. 40, 513–525.

Bary-Soroker, H., Diamant, H., 2006. Surface relaxation of lyotropic lamellar phases. Europhys. Lett. 73, 871–877.

Bary-Soroker, H., Diamant, H., 2007. Nanoscale surface relaxation of a membrane stack. Phys. Rev. E 76, 042401(1)–042401(4).

Baumgart, T., Hess, S.T., Webb, W.W., 2003. Imaging coexisting fluid domains in biomembrane models coupling curvature and line tension. Nature 425, 821–824.

Bayerl, T., 2000. Collective membrane motions. Curr. Opin. Coll. Inter. Sci. 5, 232–236.

Belrhali, H., Nollert, P., Royant, A., Menzel, C., Rosenbusch, J.P., Landau, E.M., Pebay-Peyroula, E., 1999. Protein, lipid and water organization in bacteriorhodopsin crystals: a molecular view of the purple membrane at 1.9 Å resolution. Structure 7, 909–917.

Betts, M.J., Russell, R., 2007. The hard cell: from proteomics to a whole cell model. FEBS Lett. 581, 2870–2876.

Bezrukov, M., Vodyanoy, I., 1997. Signal transduction across alamethicin ion channels in the resence of noise. Biophys. J. 73, 2456–2464.

Biscari, P., Bisi, F., 2002. Membrane-mediated interactions of rod-like inclusions Eur. Phys. J. E 6, 381–386.

Blaurock, A.E., McIntosh, T.J., 1986. Structure of the crystalline bilayers in the subgel phase of dipalmitoylphosphatidylglycerol. Biochemistry 25, 299–305.

Bloom, M., Bayerl, T., 1995. Membranes studied using neutron scattering and NMR. Can. J. Phys. 73, 687–696.

Böckmann, R.A., Hac, A., Heimburg, T., Grubmuller, H., 2003. Effect of sodium chloride on a lipid bilayer. Biophys. J. 85, 1647–1655.

Bohinc, K., Kralj-Iglič, V., May, S., 2003. Interaction between two cylindrical inclusions in a symmetric lipid bilayer. J. Chem. Phys. 119, 7435–7444.

Büldt, G., Gally, H.U., Seelig, A., Seelig, J., Zaccai, G., 1978. Neutron diffraction studies on selectively deuterated phospholipid bilayers. Nature 271, 182–184.

Caillé, A., 1972. Remarques sur la diffusion des rayons X dans les smectiques. C. R. Acad. Sci. Paris Série B 274, 891–893.

Cantor, R.S., 1997. The lateral pressure profile in membranes: a physical mechanism of general anesthesia. Biochemistry 36, 2339–2344.

Chapman, D., Byrne, P., Shipley, G.G., 1966. The physical properties of phospholipids I. Solid state and mesomorphic properties of some 2,3-diacyl-DL-phosphatidylethanolamines. Proc. Roy. Soc. A 290, 115–142.

Chapman, D., Fluck, D.J., 1966. Physical studies of phospholipids: III. Electron microscope studies of some pure fully saturated 2,3-diacyl-dl-phosphatidylethanolamines and phosphatidyl-cholines. J. Cell Biol. 30, 1–11.

Chapman, D., Morrison, A., 1966. Physical studies of phospholipids: IV. High resolution nuclear magnetic resonance spectra of phospholipids and related substances. J. Biol. Chem. 241, 5044–5052.

Chapman, D., Salsbury, N.J., 1966. Physical studies of phospholipids: V. Proton magnetic resonance studies of molecular motion in some 2,3-diacyl-dl-phosphatidylethanolamines. Trans. Faraday Soc. 62, 2607–2621.

Chapman, D., Williams, R.H., Ladbrooke, B.D., 1967. Physical studies on phospholipids. IV. Thermotropic and lyotropic mesomorphism of some 1,2-diacyl-phosphatidylcholines (lecithins). Chem. Phys. Lipids 1, 445–475.

Chapman, D., Urbina, J., Keough, K.J., 1974. Biomembrane phase transitions: studies of lipid-water systems using differential scanning calorimetry. J. Biol. Chem. 249, 2512–2521.

Chen, S.C., Sturtevant, J.M., Gaffney, B.J., 1980. Scanning calorimetric evidence for a third phase transition in phosphatidylcholine bilayers. Proc. Natl. Acad. Sci. USA 77, 5060–5063.

Chen, S., Liao, C., Huang, H., Weiss, T., Bellisent-Funel, M., Sette, F., 2001. Collective dynamics in fully hydrated phospholipid bilayers studied by inelastic X-ray scattering. Phys. Rev. Lett. 86, 740–743.

Cherezov, V., Clogston, J., Papiz, M.Z., Caffrey, M., 2006. Room to move: crystallizing membrane proteins in swollen lipidic mesophases. J. Mol. Biol. 357, 1605–1618.

Chu, N., Kučerka, N., Liu, Y., Tristram-Nagle, S., Nagle, J., 2005. Anomalous swelling of lipid bilayer stacks is caused by softening of the bending modulus. Phys. Rev. E 71, 041904.

Cusak, S., Ruigrok, R.W., Krygsman, P.C., Mellema, J.E., 1985. Structure and composition of influenza virus A small-angle neutron scattering study. J. Mol. Biol. 186, 565–582.

de Gennes, P.G., Prost, J., 1993. The Physics of Liquid Crystals. Oxford University Press, New York.

Dan, N., Pincus, P., Safran, S., 1993. Membrane-induced interactions between inclusions. Langmuir 9, 2768–2771.

Ealick, S.E., 2000. Advances in multiple wavelength anomalous diffraction crystallography. Curr. Opin. Chem. Biol. 4, 495–499.

Evans, E.A., Parsegian, V.A., 1986. Thermal-mechanical fluctuations enhance repulsion between bimolecular layers. Proc. Natl. Acad. Sci. USA 83, 7132–7136.

Feigenson, G.W., Buboltz, J.T., 2001. Ternary phase diagram of dipalmitoyl-PC/dilauroyl-PC/cholesterol: nanoscopic domain formation driven by cholesterol. Biophys. J. 80, 2775–2788.

Fenimore, P., Frauenfelder, H., McMahon, B., Young, R., 2004. Bulk-solvent and hydration-shell fluctuations, similar to alpha- and beta-fluctuations in glasses, control protein motions and functions. Proc. Natl. Acad. Sci. USA 101, 14408–14413.

Fitter, J., Gutberlet, T., Katsaras, J. (Eds.), 2006. Neutron Scattering in Biology: Techniques and Applications. Springer, Berlin.

Frauenfelder, H., Sligar, S., Wolynes, P., 1991. The energy landscapes and motions of proteins. Science 254, 1598–1603.

Franks, N.P., 1976. Structural analysis of hydrated egg lecithin and cholesterol bilayers: I X-ray diffraction. J. Mol. Biol. 100, 345–358.

Author's personal copy

Franks, N.P., Arunachalam, T., Caspi, E., 1978. A direct method for determination of membrane electron density profiles on an absolute scale. Nature 276, 530–532.

Fox, R.O., Richards, F.M., 1982. A voltage-gated ion channel model inferred from the crystal structure of alamethicin at 1.5 Å resolution. Nature 300, 325–330.

Gandhavadi, M., Allende, D., Vidal, A., Simon, S.A., McIntosh, T.J., 2002. Structure, composition, and peptide binding properties of detergent soluble bilayers and detergent resistant rafts. Biophys. J. 82, 1469–1482.

Gavin, A.C., Superti-Furga, G., 2003. Protein complexes and proteome organization from yeast to man. Curr. Opin. Chem. Biol. 7, 21–27.

Goodsaid-Zalduondo, F., Rintoul, D.A., Carlson, J.C., Hansel, W., 1982. Luteolysis-induced changes in phase composition and fluidity of bovine luteal cell membranes. Proc. Natl. Acad. Sci. USA 79, 4332–4336.

Gorter, E., Grendel, F., 1925. On bimolecular layers of lipoids on the chromocytes of the blood. J. Exp. Med. 41, 439–443.

Hammermann, M., Brun, N., Klenin, K.V., May, R., Tóth, K., Langowski, J., 1998. Salt-dependent DNA superhelix diameter studied by small angle neutron scattering measurements and Monte Carlo simulations. Biophys. J. 75, 3057–3063.

Harbich, W., Helfrich, W., 1984. The swelling of egg lecithin in water. Chem. Phys. Lipids 36, 39–63.

Harroun, T.A., Koslowsky, M., Nieh, M.-P., de Lannoy, C.-F., Raghunathan, V.A., Katsaras, J., 2005. Comprehensive examination of mesophases formed by DMPC and DHPC mixtures. Langmuir 21, 5356–5361.

Harroun, T.A., Katsaras, J., Wassall, S.R., 2006. Cholesterol hydroxyl group is found to reside in the center of a polyunsaturated lipid membrane. Biochemistry 25, 1227–1233.

Harroun, T.A., Katsaras, J., Wassall, S.R., 2008. Cholesterol is found to reside in the center of a polyunsaturated lipid membrane. Biochemistry 47, 7090–7096.

Haupts, U., Tittor, J., Oesterhelt, D., 1999. Closing in on bacteriorhodopsin: Progress in understanding the molecule. Annu. Rev. Biophys. Biomol. Struct. 28, 367–399.

Hayward, J.A., Smith, J.C., 2002. Temperature dependence of protein dynamics: Computer simulation analysis of neutron scattering properties. Biophys. J. 82, 1216–1225.

He, K., Ludtke, S.J., Heller, W.T., Huang, H.W., 1996. Mechanism of alamethicin insertion into lipid bilayers. Biophys. J. 71, 2669–2679.

Heberle, J., Büldt, G., Koglin, E., Rosenbusch, J.P., Landau, E.M., 1998. Assessing the functionality of a membrane protein in a three-dimensional crystal. J. Mol. Biol. 281, 587–592.

Helfrich, W., 1973. Elastic properties of lipid bilayers: Theory and possible experiments. Z. Naturforsch. 28c, 693–703.

Heller, W.T., He, K., Ludtke, S.J., Harroun, T.A., Huang, H.W., 1997. Effect of changing the size of lipid headgroup on peptide insertion into membrane. Biophys. J. 73, 239–244.

Hildenbrand, M.F., Bayerl, T.M., 2005. Differences in the modulation of collective membrane motions by ergosterol, lanosterol, and cholesterol: a dynamic light scattering study. Biophys. J. 88, 3360–3367.

Hirn, R., Bayerl, T.M., Rädler, J., Sackmann, E., 1999. Collective membrane motions of high and low amplitude, studied by dynamic light scattering and micro-interferometry. Faraday Discuss. 111, 17–30.

Hirn, R.B., Bayerl, T.M., 1999. Collective membrane motions in the mesoscopic range and their modulation by the binding of a monomolecular protein layer of streptavidin studied by dynamic light scattering. Phys. Rev. E 59, 5987–5994.

Hodzic, A., Rappolt, M., Amenitsch, H., Laggner, P., Pabst, G., 2008. Differential modulation of membrane structure and fluctuation by plant sterols and cholesterol. Biophys. J. 94, 3935–3944.

Horton, M.R., Reich, C., Gast, A.P., Rädler, J.O., Nickel, B., 2007. Structure and dynamics of crystalline protein layers bound to supported lipid bilayers. Langmuir 23, 6263–6269.

Huang, H.W., 2006. Molecular mechanism of antimicrobial peptides: the origin of cooperativity. Biochim. Biophys. Acta. 1758, 1292–1302.

Huang, J., Buboltz, J.T., Feigenson, G.W., 1999. Maximum solubility of cholesterol in phosphatidylcholine and phosphatidylethanolamine bilayers. Biochim. Biophys. Acta 1417, 89–100.

Huang, J., Feigenson, G.W., 1999. A microscopic interaction model of maximum solubility of cholesterol lipid bilayers. Biophys. J. 76, 2142–2157.

Hwang, J.S., Oweimreen, G.A., 2003. Anomalous viscosity behavior of a bicelles system with various molar ratios of short- and long-chain phospholipids. Arab. J. Sci. Eng. 28, 43–49.

Inoko, Y., Yamaguchi, T., Furuya, K., Mitsui, T., 1975. Effects of cations on dipalmitoylphosphatidylcholine/cholesterol/water systems. Biochim. Biophys. Acta 413, 24–32.

Ipsen, J.H., Karlstrőm, G., Mouritsen, O.G., Wennerstrőm, H.W., Zuckermann, M., 1987. Phase equilibria in the phosphatidycholine-cholesterol system. Biochim. Biophys. Acta 905, 162–172.

Israelachvili, J.N., Wennerstroem, H., 1990. Hydration or steric forces between amphiphilic surfaces? Langmuir 6, 873–876.

Israelachvili, J.N., Adams, G.E., 1978. Measurement of forces between two mica surfaces in aqueous electrolyte solutions in the range 0–100 nm. J. Chem. Soc. Faraday Trans. 74, 975–1001.

Jacobson, K., Dietrich, C., 1999. Looking at lipid rafts? Trends Cell. Biol. 9, 87–91.

Jacrot, B., 1976. The study of biological structures by neutron scattering in solution. Rep. Prog. Phys. 39, 911–953.

Karmakar, S., Sarangi, B.R., Raghunathan, V.A., 2006. Phase behaviour of lipid-cholesterol membranes. Solid State Comm. 139, 630–634.

Katsaras, J., Raghunathan, V.A., Dufourc, E.J., Dufourcq, J., 1995. Evidence for a two-dimensional lattice in subgel phase DPPC bilayers. Biochemistry 34, 4684–4688.

Katsaras, J., Harroun, T.A., Pencer, J., Nieh, M.-P., 2005. Bicellar lipid mixtures as used in biochemical and biophysical studies. Naturwissenschaften 92, 355–366.

Kendrew, J., Bodo, G., Dintzis, H., Parrish, R., Wyckoff, H., Phillips, D., 1958. A three-dimensional model of the myoglobin molecule obtained by X-ray analysis. Nature 181, 662–666.

Killian, J.A., 2003. Synthetic peptides as models for intrinsic membrane proteins. FEBS Lett. 555, 134–138.

Klauda, J.B., Kučerka, N., Brooks, B.R., Pastor, R.W., Nagle, J.F., 2006. Simulation-based methods for interpreting X-ray data from lipid bilayers. Biophys. J. 90, 2796–2807.

Koltover, I., Salditt, T., Rigaud, J.-L., Safinya, C., 1998. Stacked 2D crystalline sheets of the membrane-protein bacteriorhodopsin: a specular and diffuse reflectivity study. Phys. Rev. Lett. 81, 2494–2497.

Koltover, I., Rädler, J., Salditt, T., Safinya, C., 1999. Phase behavior and interactions of the membrane-protein bacteriorhodopsin. Phys. Rev. Lett. 82, 3184–3187.

König, S., Pfeiffer, W., Bayerl, T., Richter, D., Sackmann, E., 1992. Molecular dynamics of lipid bilayers studied by incoherent quasi-elastic neutron scattering. J. Phys. II France 2, 1589–1615.

König, S., Sackmann, E., Richter, D., Zorn, R., Carlile, C., Bayerl, T., 1994. Molecular dynamics of water in oriented DPPC multilayers studied by quasielastic neutron scattering and deuterium-nuclear magnetic resonance relaxation. J. Chem. Phys. 100, 3307–3316.

König, S., Bayerl, T., Coddens, G., Richter, D., Sackmann, E., 1995. Hydration dependence of chain dynamics and local diffusion in L-alpha dipalmitoylphosphtidylcholine multilayers studied by incoherent quasi-elastic neutron scattering. Biophys. J. 68, 1871–1880.

Kralchevsky, P.A., 1997. Lateral forces acting between particles in liquid films or lipid membranes. Adv. Biophys. 34, 25–39.

Krueger, S., 2001. Neutron reflection from interfaces with biological and biomimetic materials. Curr. Opin. Coll. Inter. Sci. 6, 111–117.

Kučerka, N., Liu, Y., Chu, N., Petrache, H.I., Tristram-Nagle, S., Nagle, J.F., 2005. Structure of fully hydrated fluid phase DMPC and DLPC lipid bilayers using X-ray scattering from oriented multilamellar arrays and from unilamellar vesicles. Biophys. J. 88, 2626–2637.

Kučerka, N., Pencer, J., Sachs, J.N., Nagle, J.F., Katsaras, J., 2007. Curvature effect on the structure of phospholipid bilayers. Langmuir 23, 1292–1299.

Kučerka, N., Nagle, J.F., Sachs, J.N., Feller, S.E., Pencer, J., Jackson, A., Katsaras, J., 2008a. Lipid bilayer structure determined by the simultaneous analysis of neutron and X-ray scattering data. Biophys. J. 95, 2356–2367.

Kučerka, N., Szabo, E., Nieh, M.-P., Harroun, T.A., Schooling, S.R., Pencer, J., Nicholson, E.A., Beveridge, T.J., Katsaras, J., 2008b. Effect of cations on the structure of bilayers formed by lipopolysaccharides isolated from p. aeruginosa PAO1. J. Phys. Chem. B 112, 8057–8062.

Kučerka, N., Marquardt, D., Harroun, T.A., Nieh, M.-P., Wassall, S.R., Katsaras, J., 2009a. The functional significance of lipid diversity: orientation of cholesterol in bilayers is determined by lipid species. J. Am. Chem. Soc. 131, 16358–16359.

Kučerka, N., Gallová, J., Uhríková, D., Balgavý, P., Bulacu, M., Marrink, S.J., Katsaras, J., 2009b. Areas of monounsaturated diacylphosphatidylcholines. Biophys. J. 97, 1926–1932.

Kučerka, N., Nieh, M.-P., Katsaras, J., 2009c. Asymmetric distribution of cholesterol in unilamellar vesicles of monounsaturated phospholipids. Langmuir 25, 13522–13527.

Kunz, W., Lo Nostro, P., Ninham, B.W. (Eds.), 2004. Hofmeister Phenomena. Curr. Opin. Colloid Interface Sci. 9, 9–197.

Kurkal-Siebert, V., Agarwal, R., Smith, J.C., 2008. Hydration-dependent dynamical transition in protein: Protein interactions at ~240 K. Phys. Rev. Lett. 100, 138102(1)–138102 (4).

Lagüe, P., Zuckermann, M.J., Roux, B., 2001. Lipid-mediated interactions between intrinsic membrane proteins: dependence on protein size and lipid composition. Biophys. J. 81, 276–284.

Landau, E.M., Rosenbusch, J.P., 1996. Lipidic cubic phases: a novel concept for the crystallization of membrane proteins. Proc. Natl. Acad. Sci. USA 93, 14532–14535.

Landau, E., Rummel, G., Cowan-Jacob, S.W., Rosenbusch, J.P., 1997. Crystallisation of a polar protein and small molecules from the aqueous compartment of lipidic cubic phases. J. Phys. Chem. B 101, 1935–1937.

Langmuir, I., 1917. The constitution and fundamental properties of solids and liquids II. Liquids. J. Am. Chem. Soc. 39, 1848–1906.

Lanyi, J., 2004. Bacteriorhodopsin. Annu. Rev. Physiol. 66, 665–688.

Ledere, H., May, R.P., KJEMS, J.K., Baer, G., 2005. Solution structure of a short DNA fragment studied by neutron scattering. Eur. J. Biochem. 161, 191–196.

Lee, M.T., Chen, F.Y., Huang, H.W., 2004. Energetics of pore formation induced by antimicrobial peptides. Biochemistry 43, 3590–3599.

Lei, N., Safinya, C.R., Bruinsma, R.F., 1995. Discrete harmonic model for stacked membranes: theory and experiment. J. Phys. II 5, 1155–1163.

Léonard, A., Escrive, C., Laguerre, M., Pebay-Peyroula, E., Néri, W., Pott, T., Katsaras, J., Dufourc, E.J., 2001. Location of cholesterol in DMPC membranes. A comparative study by neutron diffraction and molecular dynamics simulation. Langmuir 17, 2019–2030.

Lindahl, E., Edholm, O., 2000. Mesoscopic undulations and thickness fluctuations in lipid bilayers from molecular dynamics simulations. Biophys. J. 79, 426–433.

Lipowsky, R., Leibler, S., 1986. Unbinding transition of interacting membranes. Phys. Rev. Lett. 56, 2541–2544.

Lipowsky, R., Sackmann, E. (Eds.), 1995. Structure and Dynamics of Membranes. Elsevier.

Author's personal copy

Lis, L.J., Rand, R.P., Parsegian, V.A., 1980. Measurement of the absorption of Ca^{2+} and Mg^{2+} to phosphatidylcholine bilayers. Bioelectrochem 2, 41–47.

Lis, L.J., Lis, W.T., Parsegian, V.A., Rand, R.P., 1981. Adsorption of divalent cations to a variety of phosphatidylcholine bilayers. Biochemistry 20, 1771–1777.

Liu, W., Teng, T.Y., Wu, Y., Huang, H.W., 1991. Phase determination for membrane diffraction by anomalous dispersion. Acta Crystallogr. A 47, 553–559.

Liu, Y., Nagle, J.F., 2004. Diffuse scattering provides material parameters and electron density profiles of biomembranes. Phys. Rev. E 69, 040901(1)–040901(4).

Liu, D., Chu, X.-Q., Lagi, M., Zhang, Y., Fratini, E., Baglioni, P., Alatas, A., Said, A., Alp, E., Chen, S.-H., 2008. Studies of phononlike low-energy excitations of protein molecules by inelastic X-ray scattering. Phys. Rev. Lett. 101, 135501(1)–135501(4).

Loosely-Millman, M.E., Rand, R.P., Parsegian, V.A., 1982. Effects of monovalent ion binding and screening on measured electrostatic forces between charged phospholipid bilayers. Biophys. J. 40, 221–232.

Losonczi, J.A., Prestegard, J.H., 1998. Improved dilute bicelle solutions for high-resolution NMR of biological macromolecules. J. Biomol. NMR. 12, 447–451.

Luecke, H., Richter, H.T., Lanyi, J.K., 1998. Proton transfer pathways in bacteriorhodopsin at 2.3 Å resolution. Science 280, 1934–1937.

Luecke, H., Schobert, B., Richter, H.T., Cartailler, J.P., Lanyi, J.K., 1999a. Structure of bacteriorhodopsin at 1.55 Å resolution. J. Mol. Biol. 291, 899–911.

Luecke, H., Schobert, B., Richter, H.-T., Cartailler, J.-P., Lanyi, J.K., 1999b. Structural changes in bacteriorhodopsin during ion transport at 2 Å resolution. Science 286, 255–260.

Lundstrom, K., 2004. Structural genomics on membrane proteins: mini review. Comb. Chem. High Throughput Screen 7, 431–439.

Lundstrom, K., 2006. Structural genomics for membrane proteins. Cell. Mol. Life Sci. 63, 2597–2607.

Luzzati, V., Tardieu, A., Taupin, D., 1972. A pattern-recognition approach to the phase problem: application to the X-ray diffraction study of biological membranes and model systems. J. Mol. Biol. 64, 269–286.

Lyatskaya, Y., Liu, Y., Tristram-Nagle, S., Katsaras, J., Nagle, J.F., 2001. Method for obtaining structure and interactions from oriented lipid bilayers. Phys. Rev. E 63, 011907(1)–011907(9).

Mahabir, S., Wan, W.K., Katsaras, J., Nieh, M.-P. The effects of charge density and thermal path on the morphologies of spontaneously formed unilamellar vesicles. J. Phys. Chem. B., in press.

Marčelja, S., Radić, N., 1976. Repulsion of interfaces due to boundary water. Chem. Phys. Lett. 42, 129–130.

Marrink, S.J., Risselada, H.J., Yefimov, S., Tieleman, D.P., de Vries, A.H., 2007. The MARTINI force field: coarse grained model for biomolecular simulations. J. Phys. Chem. B. 111, 7812–7824.

Marrink, S.J., de Vries, A.H., Harroun, T.A., Katsaras, J., Wassall, S.R., 2008. Cholesterol shows preference for the interior of polyunsaturated lipid membranes. J. Am. Chem. Soc. 130, 10–11.

Mason, P.C., Nagle, J.F., Epand, R.M., Katsaras, J., 2001. Anomalous swelling in phospholipid bilayers is not coupled to the formation of a ripple phase. Phys. Rev. E 63, 030902(1)–030902(4).

McGillivray, D.J., Valincius, G., Vanderah, D.J., Febo-Ayala, W., Woodward, J.T., Heinrich, F., Kasianowicz, J.J., Lösche, M., 2007. Molecular-scale structural and functional characterization of sparsely tethered bilayer membranes. Biointerphases 2, 21–33.

McIntosh, T.J., Simon, S.A., 1986. Hudration force and bilayers deformation: a reevaluation. Biochemistry 25, 4058–4066.

McIntosh, T.J., Magid, A.D., Simon, S.A., 1987. Steric interaction between phosphocholine bilayers. Biochemistry 26, 7325–7332.

McIntosh, T.J. (Ed.), 2007. Lipid Rafts. Methods in Molecular Biology, vol. 398. Humana Press.

Meinhold, L., Smith, J.C., Kitao, A., Zewail, A.H., 2007. Picosecond fluctuating protein energy landscape mapped by pressure–temperature molecular dynamics simulation. Proc. Natl. Acad. Sci. USA 104, 17261–17265.

Mezei, F. (Ed.), 1980. Neutron Spin Echo. Springer.

Mills, T.T., Toombes, G.E., Tristram-Nagle, S., Smilgies, D.M., Feigenson, G.W., Nagle, J.F., 2008. Order parameters and areas in fluid-phase oriented lipid membranes using wide angle X-ray scattering. Biophys. J. 94, 117–124.

Mills, T.T., Huang, J., Feigenson, G.W., Nagle, J.F., 2009. Effects of cholesterol and unsaturated DOPC lipid on chain packing of saturated gel-phase DPPC bilayers. Gen. Physiol. Biophys. 28, 126–139.

Nagle, J.F., Tristram-Nagle, S., 2000. Structure of lipid bilayers. Biochim. Biophys. Acta 1469, 159–195.

Nakada, C., Ritchie, K., Oba, Y., Nakamura, M., Hotta, Y., Iino, R., Kasai, R.S., Yamaguchi, K., Fujiwara, T., Kusumi, A., 2003. Accumulation of anchored proteins forms membrane diffusion barriers during neuronal polarization. Nat. Cell Biol. 5, 626–632.

Neutze, R., Pebay-Peyroula, E., Royant, A., Navarro, J., Landau, E., 2002. Bacteriorhodopsin: a high resolution structural view of vectorial proton transport. Biochim. Biophys. Acta 1565, 144–167.

Nevzorov, A., Brown, M., 1997. Bilayers from comparative analysis of ^{2}H and ^{13}C NMR relaxation data as a function of frequency and temperature. J. Chem. Phys. 107, 10288–10310.

Nieh, M.-P., Glinka, C.J., Krueger, S., Prosser, R.S., Katsaras, J., 2001. SANS study of the structural phases of magnetically alignable lanthanide-doped phospholipid mixtures. Langmuir 17, 2629–2638.

Nieh, M.-P., Glinka, C.J., Krueger, S., Prosser, R.S., Katsaras, J., 2002. SANS study on the effect of lanthanide ions and charged lipids on the morphology of phospholipid mixtures. Biophys. J. 82, 2487–2498.

Nieh, M.-P., Raghunathan, V.A., Wang, H., Katsaras, J., 2003. Highly aligned lamellar lipid domains induced by macroscopic confinement. Langmuir 19, 6936–6941.

Nieh, M.-P., Raghunathan, V.A., Glinka, C.J., Harroun, T.A., Pabst, G., Katsaras, J., 2004. Magnetically alignable phase of phospholipid "bicelles" mixtures is a chiral nematic made up of wormlike micelles. Langmuir 20, 7893–7897.

Nieh, M.-P., Raghunathan, V.A., Glinka, C.J., Harroun, T.A., Katsaras, J., 2005a. Structural phase behavior of high-concentration, alignable biomimetic "bicelle mixtures. Macromol. Symp. 219, 135–145.

Nieh, M.-P., Raghunathan, V.A., Kline, S.R., Harroun, T.A., Huang, C.-Y., Pencer, J., Katsaras, J., 2005b. Spontaneously formed unilamellar vesicles with path-dependent size distribution. Langmuir 21, 6656–6661.

Nieh, M.-P., Katsaras, J., Qi, X., 2008. Controlled release mechanisms of spontaneously forming unilamellar vesicles. Biochim. Biophys. Acta – Biomembranes 1778, 1467–1471.

Nieh, M.-P., Kučerka, N., Katsaras, J., 2009. Spontaneously formed unilamellar vesicles. Meth. Enzymol. 465, 3–20.

Pabst, G., Rappolt, M., Amenitsch, H., Laggner, P., 2000. Structural information from multilamellar liposomes at full hydration: full q-range fitting with high quality X-ray data. Phys. Rev. E 62, 4000–4009.

Pabst, G., Katsaras, J., Raghunathan, V.A., 2002. Enhancement of steric repulsion with temperature in oriented lipid multilayers. Phys. Rev. Lett. 88, 128101(1)–128101(4).

Pabst, G., Katsaras, J., Raghunathan, V.A., Rappolt, M., 2003. Structure and interactions in the anomalous swelling regime of phospholipid bilayers. Langmuir 19, 1716–1722.

Pabst, G., Danner, S., Podgornik, R., Katsaras, J., 2007a. Entropy-driven softening of fluid lipid bilayers by alamethicin. Langmuir 23, 11705–11711.

Pabst, G., Danner, S., Karmakar, S., Deutsch, G., Raghunathan, V.A., 2007b. On the propensity of phosphatidylglycerols to form interdigitated phases. Biophys. J. 93, 513–525.

Pabst, G., Hodzic, A., Strancar, J., Danner, S., Rappolt, M., Laggner, P., 2007c. Rigidification of neutral lipid bilayers in the presence of salts. Biophys. J. 93, 2688–2696.

Pabst, G., Grage, S.L., Danner-Pongratz, S., Jing, W., Ulrich, A.S., Watts, A., Lohner, K., Hickel, A., 2008. Membrane thickening by the antimicrobial peptide PGLa. Biophys. J. 95, 5779–5788.

Pabst, G., Boulgaropoulos, B., Gander, E., Sarangi, B.R., Amentisch, H., Raghunathan, V.A., Laggner, P., 2009. Effect of ceramide on nonraft proteins. J. Membrane Biol. 231, 125–132.

Pan, D., Wang, W., Liu, W., Yang, L., Huang, H.W., 2006. Chain packing in the inverted hexagonal phase of phospholipids: a study by X-ray anomalous diffraction on bromine-labeled chains. J. Am. Chem. Soc. 128, 3800–3807.

Pan, J., Mills, T.T., Tristram-Nagle, S., Nagle, J.F., 2008a. Cholesterol perturbs lipid bilayers nonuniversally. Phys. Rev. Lett. 100, 198103(1)–198103(4).

Pan, J., Tristram-Nagle, S., Kučerka, N., Nagle, J.F., 2008b. Temperature dependence of structure, bending rigidity and bilayer interactions of DOPC bilayers. Biophys. J. 94, 117–124.

Pan, J., Tieleman, P.D., Nagle, J.F., Kučerka, N., Tristram-Nagle, S., 2009. Alamethicin in lipid bilayers: combined use of X-ray scattering and MD simulations. Biochim. Biophys. Acta 1788, 1387–1397.

Parfait, R., Koch, M.H.J., Stuhrmann, H.B., Crichton, R.R., 1978. Ribosome structure studies by low angle neutron scattering. Trends Biol. Sci. 3, 41–43.

Parsegian, V.A., Rand, R.P., Fuller, N.L., Rau, D.C., 1986. Methods in Enzymology, Vol. 127. Academic Press, New York.

Parsegian, V.A., Rand, R.P., 1991. On molecular protrusion as the source of hydration forces. Langmuir 7, 1299–1301.

Parsegian, V.A., 2006. Van der Waals Forces: A Handbook for Biologists, Chemists, Engineers, and Physicists. Cambridge University Press.

Pawson, T., Nash, P., 2003. Assembly of cell regulatory systems through protein interaction domains. Science 300, 445–452.

Pebay-Peyroula, E., Rummel, G., Rosenbusch, J.P., Landau, E.M., 1997. X-ray structure of bacteriorhodopsin at 2.5 Å from microcrystals grown in lipidic cubic phases. Science 277, 1676–1681.

Pencer, J., Mills, T., Anghel, V.N.P., Krueger, S., Epand, R.M., Katsaras, J., 2005. Detection of submicron-sized raft-like domains in membranes by small-angle neutron scattering. Eur. Phys. J. E 18, 447–458.

Pencer, J., Anghel, V.N.P., Kučerka, N., Katsaras, J., 2006. Scattering from laterally heterogeneous vesicles I: model independent analysis. J. Appl. Cryst. 39, 791–796.

Pencer, J., Anghel, V.N.P., Kučerka, N., Katsaras, J., 2007. Scattering from laterally heterogeneous vesicles III. Reconciling past and present work. J. Appl. Cryst. 40, 771–772.

Pencer, J., Jackson, A., Kučerka, N., Nieh, M.-P., Katsaras, J., 2008. The influence of curvature on membrane domains. Eur. Biophys. J. 37, 665–671.

Petrache, H., Gouliaev, N., Tristram-Nagle, S., Zhang, R., Suter, R.M., Nagle, J.F., 1998. Interbilayer interactions from high-resolution X-ray scattering. Phys. Rev. E 57, 7014–7024.

Petrache, H.I., Kimchi, I., Harries, D., Parsegian, V.A., 2005. Measured depletion of ions at the biomembrane interface. J. Am. Chem. Soc. 127, 11546–11547.

Petrache, H.I., Tristram-Nagle, S., Harries, D., Kučerka, N., Nagle, J.F., Parsegian, V.A., 2006a. Swelling of phospholipids by monovalent salt. J. Lipid Res. 47, 302–309.

Petrache, H.I., Zemb, T., Belloni, L., Parsegian, V.A., 2006b. Salt screening and specific ion adsorption determine neutral-lipid membrane interactions. Proc. Natl. Acad. Sci. USA 103, 7982–7987.

Pfeiffer, W., Henkel, T., Sackmann, E., Knorr, W., 1989. Local dynamics of lipid bilayers studied by incoherent quasi-elastic neutron scattering. Europhys. Lett. 8, 201–206.

Author's personal copy

Pfeiffer, W., König, S., Legrand, J., Bayerl, T., Richter, D., Sackmann, E., 1993. Neutron spin echo study of membrane undulations in lipid multibilayers. Europhys. Lett. 23, 457–462.

Pockels, A., 1894. On the spreading of oil upon water. Nature 50, 223–224.

Podgornik, R., Parsegian, V.A., 1992. Thermal mechanical fluctuations of fluid membranes in confined geometries – the case of soft confinement. Langmuir 8, 557–562.

Pozo-Navas, B., Raghunathan, V.A., Katsaras, J., Rappolt, M., Lohner, K., Pabst, G., 2003. Discontinuous unbinding of lipid multibilayers. Phys. Rev. Lett. 91, 028101(1)–028101(4).

Pozo-Navas, B., Lohner, K., Deutsch, G., Sevcsik, E., Riske, K., Dimova, A., Garidel, R., Pabst, P.G., 2005. Composition dependence of vesicle morphology and mixing properties in a bacterial model membrane system. Biochim. Biophys. Acta 1716, 40–48.

Prosser, R.S., Volkov, V.B., Shiyanovskaya, I.V., 1998a. Novel chelate-induced magnetically alignment of biological membranes. Biophys. J. 75, 2163–2169.

Prosser, R.S., Volkov, V.B., Shiyanovskaya, I.V., 1998b. Solid-state NMR studies of magnetically aligned phospholipid membranes: taming lanthanides for membrane protein studies. Biochem. Cell Biol. 76, 443–451.

Raffard, G., Steinbruchner, S., Arnold, A., Davis, J.H., Dufourc, E.J., 2000. Temperature-composition diagram of dimyristoylphosphatidylcholine-dicaproylphosphatidylcholine "bicelles" self-orienting in magnetic field. A solid state ^{2}H and ^{31}P NMR study. Langmuir 16, 7655–7662.

Raghunathan, V.A., Katsaras, J., 1995. Structure of the $L_{c'}$ phase in a hydrated lipid multilamellar system. Phys. Rev. Lett. 74, 4456–4459.

Raghunathan, V.A., Katsaras, J., 1996. L_{β}'–L_{c}' phase transition in phosphatidylcholine bilayers: a disorder–order transition in two dimensions. Phys. Rev. E 54, 4446–4449.

Rand, R.P., Parsegian, V.A., 1989. Hydration forces between phospholipid bilayers. Biochim. Biophys. Acta 988, 351–376.

Rappolt, M., 2006. The biologically relevant lipid mesophases as "seen" by X-rays. In: Leitmannova-Liu, A. (Ed.), Advances in Planar Lipid Bilayers and Liposomes, Vol. 5. Elsevier, Amsterdam, pp. 253–283.

Rappolt, M., Pabst, G., 2008. Flexibility and structure of fluid bilayer interfaces. In: Nag, K. (Ed.), Structure and Dynamics of Membranous Interfaces. Wiley, Hoboken (NJ) USA, pp. 45–81.

Rawicz, W., Olbrich, K.C., McIntosh, T., Needham, D., Evans, E., 2000. Effect of chain length and unsaturation on elasticity of lipid bilayers. Biophys. J. 79, 328–339.

Rheinstädter, M.C., Ollinger, C., Fragneto, G., Demmel, F., Salditt, T., 2004. Collective dynamics of lipid membranes studied by inelastic neutron scattering. Phys. Rev. Lett. 93, 108107(1)–108107(4).

Rheinstädter, M.C., Seydel, T., Demmel, F., Salditt, T., 2005. Molecular motions in lipid bilayers studied by the neutron backscattering technique. Phys. Rev. E71, 061908(1)–061908(8).

Rheinstädter, M.C., Häussler, W., Salditt, T., 2006a. Dispersion relation of lipid membrane shape fluctuations by neutron spin-echo spectrometry. Phys. Rev. Lett. 97, 048103(1)–048103(4).

Rheinstädter, M.C., Seydel, T., Häußler, W., Salditt, T., 2006b. Exploring the collective dynamics of lipid membranes with inelastic neutron scattering. J. Vac. Sci. Technol. A 24, 1191–1196.

Rheinstädter, M.C., Seydel, T., Farago, B., Salditt, T., 2006c. Probing dynamics at interfaces: options for neutron and X-ray spectroscopy. J. Neutron Res. 14, 257–268.

Rheinstädter, M.C., Seydel, T., Salditt, T., 2007. Nanosecond molecular relaxations in lipid bilayers studied by high energy resolution neutron scattering and in-situ diffraction. Phys. Rev. E 75, 011907(1)–011907(8).

Rheinstädter, M.C., Das, J., Flenner, E.J., Brüning, B., Seydel, T., Kosztin, I., 2008a. Motional coherence in fluid phospholipid membranes. Phys. Rev. Lett. 101, 248106(1)–248106(4).

Rheinstädter, M.C., 2008b. Collective molecular dynamics in proteins and membranes. Biointerphases 3 (2), FB83–FB90.

Rheinstädter, M.C., Schmalzl, K., Wood, K., Strauch, D., 2009. Protein–protein interaction in purple membrane, Phys. Rev. Lett. 103, 128104(1)–128104(4).

Romanov, V.P., Ul'yanov, S.V., 2002. Dynamic and correlation properties of solid supported smectic-a films. Phys. Rev. E 66, 061701(1)–061701(9).

Ribotta, R., Salin, D., Durand, G., 1974. Quasielastic Rayleigh scattering in a smectic – a crystal. Phys. Rev. Lett. 32, 6–9.

Rummel, G., Hardmeyer, A., Widmer, C., Chiu, M., Nollert, P., Locher, K., Pedruzzi, I., Landau, E.M., Rosenbusch, J.P., 1998. Lipidic cubic phases: new matrices for the three-dimensional crystallization of membrane proteins. J. Struct. Biol. 121, 82–91.

Ruocco, M.J., Shipley, G.G., 1982a. Characterization of the sub-transition of hydrated dipalmitoylphosphatidylcholine bilayers: X-ray diffraction study. Biochim. Biophys. Acta 684, 59–66.

Ruocco, M.J., Shipley, G.G., 1982b. Characterization of the sub-transition of hydrated dipalmitoylphosphatidylcholine bilayers kinetic, hydration and structural study. Biochim. Biophys. Acta 691, 309–320.

Sachs, J.N., Petrache, H.I., Woolf, T.B., 2003. Interpretation of small angle X-ray measurements guided by molecular dynamics simulations of lipid bilayers. Chem. Phys. Lipids 126, 211–223.

Salditt, T., 2000. Structure and fluctuations of highly oriented phospholipid membranes. Curr. Opin. Coll. Inter. Sci. 5, 19–26.

Salditt, T., Vogel, M., Fenzl, W., 2003. Thermal fluctuations and positional correlations in oriented lipid membranes. Phys. Rev. Lett. 90, 178101(1)–178101(4).

Salditt, T., 2005. Thermal fluctuations and stability of solid-supported lipid membranes. J. Phys. Condens. Mattrer 17, R287–R314.

Sanders II, C.R., Schwonek, J.P., 1992. Characterization of magnetically orientable bilayers in mixtures of dihexanoylphosphatidylcholine and dimyristoylphosphatidylcholine by solid-state NMR. Biochemistry 30, 8898–8905.

Sanders II, C.R., Landis, G.C., 1995. Reconstitution of membrane proteins into lipid-rich bilayered mixed micelles for NMR studies. Biochemistry 34, 4030–4040.

Satre, M., Zaccai, G., 1979. Small angle neutron scattering of *Escherichia coli* BF1-ATPase. FEBS Lett. 102, 244–248.

Seelig, J., Macdonald, P.M., Scherer, P.G., 1987. Phospholipid headg roups as sensors of electric charge in membranes. Biochemistry 26, 7535–7541.

Singer, S.J., Nicolson, G.L., 1972. The fluid mosaic model of the structure of cell membranes. Science 175, 720–731.

Simons, K., van Meer, G., 1988. Lipid sorting in epithelial cells. Biochemistry 27, 6197–6202.

Simons, K., Vaz, W.L.C., 2004. Model systems, lipid rafts, and cell membranes. Ann. Rev. Biophys. Biomol. Sci. 33, 269–295.

Smith, G.S., Sirota, E.B., Safinya, C.R., Clark, N.A., 1988. Structure of the L_{β} phases in a hydrated phosphatidylcholine multimembrane. Phys. Rev. Lett. 60, 813–816.

Smith, J.C., 1991. Protein dynamics: comparison of simulations with inelastic neutron scattering experiments. Q. Rev. Biophys. 24, 227–291.

Sternin, E., Nizza, D., Gawrisch, K., 2001. Temperature dependence of DMPC/DHPC mixing bicellar solution and its structural implication. Langmuir 17, 2610–2616.

Soong, R., Nieh, M.-P., Nicholson, E., Katsaras, J., Macdonald, P.M., 2010. Bicellar mixtures containing pluronic F68: morphology and lateral diffusion from combined SANS and PFG NMR studies. Langmuir 26, 2630–2638.

Sun, W.-J., Suter, R.M., Knewtson, M.A., Worthington, C.R., Tristram-Nagle, S., Zhang, R., Nagle, J.F., 1994. Order and disorder in fully hydrated unoriented bilayers of gel phase DPPC. Phys. Rev. E 49, 4665.

Takeda, T., Kawabata, Y., Seto, H., Komura, S., Gosh, S., Nagao, M., Okuhara, D., 1999. Neutron spin echo investigations of membrane undulations in complex fluids involving amphilphiles. J. Phys. Chem. Solids 60, 1375–1377.

Tardieu, A., Luzzati, V., Reman, F.C., 1973. Structure and polymorphism of the hydrocarbon chains of lipids: a study of lecithin-water phases. J. Mol. Biol. 75, 711–733.

Tarek, M., Tobias, D., Chen, S.-H., Klein, M., 2001. Short wavelength collective dynamics in phospholipid bilayers: a molecular dynamics study. Phys. Rev. Lett. 87, 238101(1)–238101(4).

Tarek, M., Tobias, D., 2002. Role of protein-water hydrogen bond dynamics in the protein dynamical transition. Phys. Rev. Lett. 88, 138101(1)–138101(4).

Teixeira, et al., 2008. New sources and instrumentation for neutrons in biology. Chem. Phys. 345, 133–151.

Torbet, J., Wilkins, M.H.F., 1976. X-ray diffraction studies of lecithin bilayers. J. Theor. Biol. 62, 447–458.

Tristram-Nagle, S., Petrache, H.I., Nagle, J.F., 1998. Structure and interactions of fully hydrated DOPC bilayers. Biophys. J. 75, 917–928.

Tristram-Nagle, S., Nagle, J.F., 2007. HIV-1 fusion peptide decreases bending energy, promotes curved fusion intermediates. Biophys. J. 93, 2048–2055.

Van Dam, L., Karlsson, G., Edwards, K., 2004. Direct observation and characterization of DMPC/DHPC aggregates under conditions relevant for biological solution NMR. Biochim. Biophys. Acta 1664, 241–256.

Van Dam, L., Karlsson, G., Edwards, K., 2006. Morphology of magnetically aligning DMPC/DHPC aggregates perforated sheets, not disks. Langmuir 22, 3280–3285.

Veatch, S.L., Polozov, I.V., Gawrisch, K., Keller, S.L., 2004. Liquid domains in vesicles investigated by NMR and fluorescence microscopy. Biophys. J. 86, 2910–2922.

Vist, M.R., Davis, J.H., 1990. Phase equilibria of cholesterol/dipalmitoylphosphatidylcholine mixtures: deuterium nuclear magnetic resonance and differential scanning calorimetry. Biochemistry 29, 451–464.

Vitkova, V., Méléard, P., Pott, T., Bivas, I., 2006. Alamethicin influence on the membrane bending elasticity. Eur. Biophys. J. 35, 281–286.

Vold, R.R., Prosser, R.S., Deese, A.J., 1997. Isotropic solutions of phospholipid bicelles: A new membrane mimetic for high-resolution NMR studies of polypeptides. J. Biomol. NMR 9, 329–355.

Whiles, J.A., Deems, R., Vold, R.R., Dennis, E.A., 2002. Bicelles in structure-function studies of membrane-associated proteins. Bioorg. Chem. 30, 431–442.

Wiener, M.C., White, S.H., 1991a. Fluid bilayer structure determination by the combined use of Xray and neutron diffraction I. Fluid bilayer models and the limits of resolution. Biophys. J. 59, 162–173.

Wiener, M.C., White, S.H., 1991b. Fluid bilayer structure determination by the combined use of X-ray and neutron diffraction II. "composition-space" refinement method. Biophys. J. 59, 174–185.

Wood, K., Plazanet, M., Gabel, F., Kessler, B., Oesterhelt, D., Tobias, D.J., Zaccai, G., Weik, M., 2007. Coupling of protein and hydration-water dynamics in biological membranes. Proc. Natl. Acad. Sci. USA 104, 18048–18054.

Worcester, D.L., Franks, N.P., 1976. Structural analysis of hydrated egg lecithin and cholesterol bilayers II. Neutron diffraction. J. Mol. Biol. 100, 359–378.

Yamada, N.L., Seto, H., Takeda, T., Nagao, M., Kawabata, Y., Inoue, K., 2005. SAXS, SANS and NSE studies on "unbound state" in DPPC/water/$CaCl_2$ system. J. Phys. Soc. Jpn. 74, 2853–2859.

Zhang, R., Suter, R.M., Nagle, J.F., 1994. Theory of the structure factor of lipid bilayers. Phys. Rev. E 50, 5047–5060.

Author's personal copy

Zaccai, G., Blasie, J.K., Scoenborn, B.P., 1975. Neutron diffraction studies on the location of water in lecithin model membranes. Proc. Natl. Acad. Sci. USA 72, 376–380.

Zaccai, G., Büldt, G., Seelig, A., Seelig, J., 1979. Neutron diffraction studies on phosphatidylcholine model membranes. II. Chain conformation and segmental disorder. J. Mol. Biol 134, 693–706.

Zaccai, G., 2000a. Moist and soft, dry and stiff: a review of neutron experiments on hydration-dynamics-activity relations in the purple membrane of halobacterium salinarum. Biophys. Chem. 86, 249–257.

Zaccai, G., 2000b. How soft is a protein? A protein dynamics force constant measured by neutron scattering. Science 288, 1604–1607.